Results in Engineering 29 (2026) 109719

Contents lists available at ScienceDirect

Results in Engineering

journal homepage: www.sciencedirect.com/journal/results-in-engineering

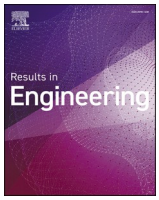

Research paper

Multi-objective optimization of CRDI engine parameters fueled with blends of diesel and sterculia foetida biodiesel: A comparative study of RSM composite desirability and meta-heuristic algorithm

Prakash Paramasivam *, Dhanasekaran C

Department of Mechanical Engineering, Vels Institute of Science, Technology and Advanced Studies (VISTAS), Pallavaram, Tamilnadu, India

ARTICLE INFO

Keywords:
Sterculia foetida biodiesel
CRDI engine
Multi objective optimization
ANN
RSM
Genetic algorithms

ABSTRACT

This study presents a comprehensive multi objective optimization of common rail direct injection (CRDI) engine parameters using response surface methodology (RSM) with composite desirability approach and three meta-heuristic algorithms: genetic algorithm with desirability function (GADF), differential evolution with desirability (DE-DF), and particle swarm optimization with desirability (PSO-DF). A central composite design (CCD) with 50 experimental runs was conducted to evaluate the effects of fuel blend percentage, engine load, injection pressure, injection timing, and EGR rate on engine performance and emissions. The study aimed to maximise torque, brake power, BMEP, brake thermal efficiency, mechanical efficiency, and volumetric efficiency while minimising specific fuel consumption, CO, HC, and NOx emissions. RSM composite desirability optimisation yielded optimal conditions at 53% fuel blend, 98% engine load, 999.97 bar injection pressure, 6.0^{o} BTDC timing, and 0% EGR. Mata-heuristic validation showed DE-DF achieving 95.3%similarity to RSM results, PSO-DF demonstrating 97.9% similarity, and GADF providing 88.9% agreement. The study validates the effectiveness of meta-heuristic algorithms as robust alternatives to traditional RSM approaches for complex engine optimization problems.

1. Introduction

Generally, fuels are used in power generation, automotive transportation, industrial, and household applications. Day by day, the necessity of fuel demand increases due to population switchover to luxurious lifestyles and industrial and technological development towards urbanisation. Therefore, in all aspects of human life, fuel plays a major role. We are currently importing fuel from other countries to satisfy our country's energy demand. Since the imported crude oil is refined to meet over three-fourths of India's energy needs, a sizeable portion of our gross domestic product is sent to other nations to purchase crude oil. The rising world energy demand, coupled with enhancing stringent atmospheric regulations, has urged intensive research into sustainable modified fuels for internal combustion engines [1]. Diesel engines are used in transportation sector due to high efficiency, nowadays biodiesel as promising alternatives for diesel fuelled engines [2].

It took almost 150 years to shape the internal combustion engine and find out the optimum input conditions of injection pressure, injection timing, spray angle, load and dimension of the engine cylinder, inlet and exhaust valve opening and closing timing by using diesel as fuel. Diesel fuel engine input parameter conditions are not suitable for biodiesel fuel, so optimization of influencing parameters of the internal combustion engine is required for alternate fuel. There are two ways to replace conventional fuel in an engine: replacement fuel can be used in blended diesel form or pure biodiesel. Hence, when this blended proportion varies, automatically the biodiesel property also varies compared with diesel fuel. Conventional diesel engine FIP and FIT are suitable only for diesel, due to the property variation of biodiesel [3,4], To use biodiesel fuel in diesel engines, primary importance should be given to parameter optimization for the sake of reducing fuel consumption and environmental degradation [5].

Nowadays CRDI engine representing the diesel engine technology due to the following nature of better fuel economy, decreased emissions, and enhanced performance compared to non CRDI diesel engines. But still, using biodiesel in internal combustion engines presents various issues, including lower engine efficiency and higher emissions; hence, optimizing engine parameters is required to minimize energy waste and emissions and to improve performance when using biodiesel blended with diesel as fuel. However, the coupling of biodiesel blends in-specific

* Corresponding author.
E-mail addresses: prakash1033@gmail.com, prakash1033.se@vistas.ac.in (P. Paramasivam).

https://doi.org/10.1016/j.rineng.2026.109719
Received 3 December 2025; Received in revised form 9 February 2026; Accepted 22 February 2026
Available online 23 February 2026

Nomenclature

SF	sterculia foetida
SS	sum of squares
ANN	artificial Neural Network
ANOVA	analysis of variance
CR	compression ratio
BP	brake power
BMEP	brake mean effective pressure
BTE	brake thermal efficiency
Vol. eff.	volumetric efficiency
SFC	specific fuel consumption
CO	carbon monoxide
HC	hydro carbon
NOx	Nitrogen oxides
TDC	top dead centre

from non-edible feedstocks of Sterculia foetida, represents complex optimization challenges that necessitate finding parameter tuning for optimal engine efficiency characteristics since existing diesel engine default design and settings suitable only for diesel fuel [6]. Explored a CRDI engine fuelled with nanoparticles-enhanced waste cooking oil biodiesel-diesel blends combined with hydrogen enrichment, comprehensively analysing performance and emission characteristics. The study recommended future research directions involving variations in IT and IP to optimize engine operation [7]. Algae biodiesel blends (B10, B15) were tested in a CRDI engine by systematically varying injection pressure from 60 to 105 MPa (in 150 bar increments) at a constant speed of 1500 rpm. Results demonstrated that peak IP operation (1050 bar) yielded reductions in specific fuel consumption, CO, and HC emissions, although accompanied by increase in NOx emissions and BTE compared to lower pressure conditions. Highlighted the challenge of substituting fossil diesel with 30–40% biodiesel blends in CRDI engines without engine hardware modifications. An optimal quaternary blend composition of diesel (60%), Cottonseed biodiesel (5), mahua biodiesel (15–20%), and n-butanol (20–15%) was identified, demonstrating improvements in BTE and HC emissions alongside reductions in SFC, CO, NOx, and smoke opacity relative to other blend configurations [8,9] Recognizing that small engines with conventional injection systems contribute significantly to emissions, modified a conventional fuel injection system to an electronically controlled CRDI configuration. Subsequent parametric studies varying CR, IP, IT enabled RSM-based optimization of engine parameters, achieving enhanced performance (improved BTE, reduced SFC) and emission profiles (lower CO, NOx, HC) [10]. A single-cylinder CRDI engine test rig facilitated identification of optimal operating conditions through RSM optimization of multiple injection parameters: main IP, start of main IT, main and pilot injection fuel quantities, and pilot IT, using neat diesel as test medium [11]. lemon peel oil biodiesel-diesel blends were systematically evaluated under various CRDI injection strategies, including variations in IP, injection rate, and pilot injection parameters. Findings revealed that

Fig. 1. processing of sterculia foetida seeds for biofuel.

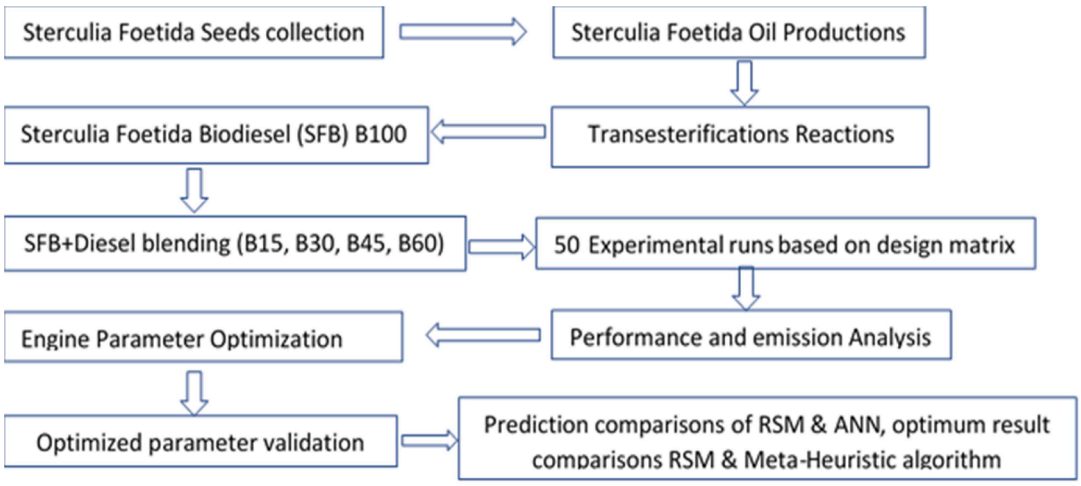

Fig. 1a. Flowchart of step-by-step methodology for CRDI engine optimization study with SFB blends.

elevated IP combined with optimized pilot injection rates consistently improved BTE across the tested conditions.

Despite biodiesel has high cetane number and flash point its viscosity and production cost is high as a result performance decreases and emissions increases [12,13]. The reason for choosing sterculia foetida (SF) biodiesel is due to its superior characteristics compared to diesel and other biodiesels, i.e., its cetane number is 54, which is higher than diesel's value of 47, and the smoke opacity of SF biodiesel is very less than diesel; in almost 50% of the diesel-sterculia foetida biodiesel blend, 45.4% of the smoke opacity was less than diesel fuel [14–16]. Also patented the production of poon oil-diesel compositions and concluded that an almost 64.5% smoke reduction was achieved for 40% SF oil and 60% diesel. Delhi, like other states, faces visibility problems in some situations due to the higher opacity around the local areas emitted by transportation vehicles. Visibility problems and health issues can be reduced by using lower-opacity Poon biodiesel. It is a non-edible and renewable oil extracted from the seeds of the poon tree, which contains 50–54% oil from the seed kernel. The cultivation of seeds happens for 5–6 months per year, usually from December to May [17–20]. Poon tree can grow anywhere, even in dry season, so it can be planted in cultivable and non-cultivable land. It grows at an altitude of more than 80 feet in a straight manner, with a depth radius of 30–60 cm and a smaller number of branches. On average, each tree produces more than 60 kg of seeds. This tree is planted in and around offices, academic institutions, and highways for decoration purposes in Tamil Nadu. Hence, it is yet to be optimised for selected SF biodiesel (also called Sterculia foetida and wild almond in different places) at different load conditions. The process of seed to biodiesel blend is shown in Fig. 1.

This fuel not competing with food security hence sustainable pathway using sterculia foetida for diesel engine applications [21]. However, the physiochemical properties of Sterculia biodiesel like higher viscosity, distinct cetane number and combustions characteristics notably influence engine operation urging comprehensive parameter optimization [22]. Biodiesel production from non-edible SF feedstock via an RSM-optimized transesterification process using Box-Behnken design achieved a maximum yield exceeding 90% at 55°C reaction temperature, 1.5% catalyst concentration, 1:12 oil-to-methanol ratio, and 900–1200 rpm stirring speed. The study also analysed performance and emissions under varying loads for SF biodiesel-diesel blends (up to B40) without injection strategy modifications [23]. RSM-based Box--Behnken design optimized oil extraction and biodiesel production from SF via transesterification, yielding 91% at 55°C, 1:12 oil-to-methanol molar ratio, 1.5% catalyst concentration, and 60 min reaction time [24]. The effect of KOH (0.8–1.2%) on SF transesterification was examined for viscosity, heating value, and density, identifying 0.8% KOH as optimal at 60°C and 1h. blending with diesel further improved these properties [25]. SF seed oil exhibits higher fatty acid content (both saturated and unsaturated) than sunflower, soybean, groundnut, or mustard oils [26]. Variations in SFB blends (B5-B30) and engine speeds (1300–2400 rpm) improved BTE (28.84%) and BSFC (5.86%) at B5, with reductions in CO (8.26%), HC (2.08%), and smoke opacity (3.08%), alongside increases in CO_2 (3.53%) and NOx (22.39%) compared to diesel. An ANN model accurately predicted engine performance and emissions [27]. Additives (dimethyl carbonate at 5–15% in constant SF B20 enhanced single-cylinder diesel engine performance and reduced emissions due to oxygen content, high volatility, and low viscosity, improving BTE and BSFC while increasing NOx and decreasing CO, HC, and smoke relative to additive-free SF B20 [28]. Reflux transesterification with 0.25% CuO-CeO_2 catalyst achieved 92% SF biodiesel yield at optimal conditions: 1:9 methanol-to-oil molar ratio, 70°C, 3h, and 600 rpm [29]. Transesterification of non-edible SF (B20) with base catalyst, followed by 5–10% n-butanol oxygenation, reduced NOx and CO2 while improving BTE compared to additive-free SF B20; CO, HC, and smoke were lower than diesel [30]. A heterogeneous catalyst from Ceiba pentandra stalks enabled esterification and transesterification of SF seed oil, yielding 97 wt% biodiesel at optimal conditions: 18:1 methanol-to-oil molar ratio, 3.5 wt % catalyst, and 498 K. based on gone through relevant literature cited and to my knowledge, no one conducted experimental work and analysed the output responses by considering all major influencing parameters in my design space study.

RSM has wide applications, its mainly useful dealing with relationship between operational parameters and outcomes are unknown or complex making traditional optimization tough. composite desirability based RSM multi parameter optimization is remains robust and statistically validated. It identifies optimal conditions with fewer experimentation [31]. Unlike AI methods requiring extensive data, traditional RSM provides interpretable surfaces, validated predictions, and minimal variance estimates, as in prior biodiesel optimizations [32,33]. RSM can effectively optimize operational parameters [34]. RSM with composite desirability have proven effective for optimization of multi objective problems. Nowadays CI engine systems comes with intricate FIT, variable valve operations, after-treatment technologies, biodiesel blend variabilities etc., which demands optimization across expansive, multimodal design spaces that surpass traditional RSM capabilities because of more non linearities among operational variables. However, the increasing complexity of modern engine systems and need for better optimization solutions have driven research toward meta heuristic algorithms capable of exploring large design spaces more effectively [35,36]. Recent advances in computational intelligence have introduced powerful meta-heuristic algorithms to handle non-linear relationship for

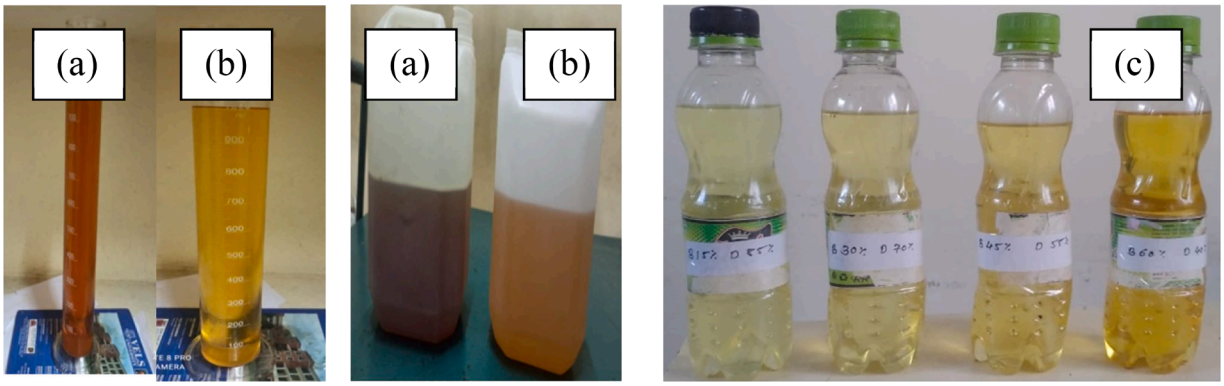

Fig. 2. (a) sterculia foetida raw oil, (b) B100, (c) biodiesel blends.

Table 1
properties of Sterculia foetida seed oil, B100 biodiesel.

Properties/ Sample	Unit	Diesel [1]	Sterculia foetida		ASTM standard
			raw oil	B100	
FFA	percentage	0.3	–	–	–
Density at 25° C	kg/m^3	816	925	877	D287
LCV	MJ/kg	42.856	36.11	40.41	D 4809
HCV	MJ/kg	45.30	38.56	42.87	D 4809
Flash Point	°C	53	219	171	D93-58T
Fire Point	°C	56	231	183	D93-58T
Kinematic Viscosity @40°C	cSt	2.09	24.3	5.93	D445
Dynamic Viscosity	cP	1.73	22.47	5.2	D445

multi objective optimization problems.

While prior research has extensively examined engine performance and emissions characteristics through individual parametric studies, and RSM has been widely applied for optimization purposes, the literature reveals a notable gap in comprehensive investigations that simultaneously evaluate multiple critical operating parameters-injection timing, EGR rate, injection pressure, brake load and biodiesel blend composition (Sterculia foetida with diesel)-within a CRDI engine operating at constant speed (1500 rpm) and CR (18:1). This study addresses that specific gap through a multi-factorial experimental design. The primary contribution involves optimizing engine settings across these five parameters using RSM with the desirability approach to simultaneously maximize BTE, vol. effi., brake power, torque, and mech. effi. while minimizing BSFC and emissions (CO, HC, NOx). As secondary contributions, the work validates RSM predictions with experimental datas against ANN models and compares the desirability-based optimization results with three meta-heuristic algorithms: genetic algorithm with desirability function (GADF), differential evolution with desirability function (DE-DF), and particle swarm optimization with desirability function (PSO-DDF).

2. Materials and methods

Figs. 1, 1a illustrates the step-by-step process of preparing SFB blends from seeds. Sterculia foetida raw oil obtained by crushing seeds in mechanical expeller and the B100 methyl ester biodiesel obtained through process called standard transesterification. The reaction was conducted at 60°C for 1 h, using SF oil to methanol molar ratio (1:12), 1.25% KOH concentration, and 800 rpm stirring speed. The various proportions of blended fuel prepared (B15, B30, B45, B60) for reducing viscosity and testing is shown in Fig. 2. Fuels are prepared based on ASTM standards and properties of calorific value and viscosity, flash and fire point etc., are shown in Table 1. Density of raw oil and biodiesel is 13.36% and 7.48% higher than diesel. The SF B100 has 3 times higher viscosity and 6% lower calorific values than regular diesel and variations in flash and

Fig. 3. (a) Experimental Setup, (b) NIRA i7r open ECU.

Table 2
Experimental setup specifications.

Engine parts	Specifications
Type	Kirloskar, 1-cylinder, 4-stroke, water-cooled CRDI VCR engine, CR (12 to 18).
swept volume	661.5 cm^3
CR (fixed)	18
Piston	hemispherical bowl
Power	at 1500 rpm is 3.5 kW
nozzle	7 hole
type of EGR	cooled by water
open ECU type	Nira i7r injector driver
type of load	an eddy current dynamometer, arm length of 185 mm
data storage and processing	IC engine software developed by apex
temperature and load sensor	PT100 and strain gauge

Table 3
Measurement range of AVL DIGAS 444N exhaust measurement instruments.

variables	Measurement range	Resolution
CO	0 to 15 % vol.	0.001% vol.
HC	0 to 20000 ppm vol	1 ppm vol.
O_2	0 to 25% vol.	0.01% vol.
CO2	0 to 20% vol.	0.1 % vol.
NOx	0 to 5000 ppm vol	1 ppm vol

Table 4
levels of impacting parameters.

			Levels				
Parameter	Unit	Factor	-2	-1	0	1	2
FB	%	A	B0	B15	B30	B45	B60
EL	kg	B	2.5	4.9	7.4	9.8	12.3
FIP	MPa	C	40	55	70	85	100
FIT	bTDC	D	6°	12°	18°	24°	30°
EGR	percent	E	0%	4%	8%	12%	16%

fire point, hence which all affecting spray, performance, emission and combustion characteristics. Blending SFB at 15%, 30%, 45%, and 60% with diesel reduces density by 5.9%, 4.9%, 3.8%, and 2.8% reduction in density compare to B100. Calorific value increases by 4.9%, 4%, 3.2%, and 2.3% relative to B100, while viscosity decreases by 55.1%, 45.4%, 35.6%, and 26% relative to B100. Due to varied spray and atomised patterns, requiring injection pressure and timing optimization. Biodiesel contains oxygen and different ignition delay nature necessitate optimized IT and EGR strategies for balanced performance-emission trade-offs. Generally, biodiesel reduces CO, HC and particulate pollutants but it often increases NOx emissions, and this may reduce power output, hence requiring multi objective optimization approaches.

3. Experimental design and methodology

The experiments were conducted on a 1-cylinder CRDI diesel engine with systematic variation of five control parameters using CCD.

Control Parameters:

Fuel Blend (%): 0–60
Engine Load (%): 20–100
Injection pressure (bar): 400–1000
Injection timing (°BTDC): 6–30
EGR rate (%): 0–16

Response Variables:

Table 4a
Design matrix [37].

Random Run Order	FB (%)	EL (fraction)	FIP (GPa)	FIT (bTDC)	EGR (fraction)
1	B30	0.60	0.070	18°	0.08
2	B45	0.80	0.055	24°	0.12
3	B45	0.40	0.085	12°	0.04
4	B45	0.40	0.055	24°	0.04
5	B45	0.40	0.055	24°	0.12
6	B45	0.40	0.085	24°	0.12
7	B15	0.80	0.055	12°	0.12
8	B45	0.80	0.085	12°	0.12
9	B45	0.80	0.085	12°	0.04
10	B15	0.40	0.085	24°	0.12
11	B30	0.60	0.070	18°	0.08
12	B45	0.40	0.085	24°	0.04
13	B45	0.40	0.085	12°	0.12
14	B15	0.40	0.055	12°	0.04
15	B45	0.40	0.055	12°	0.12
16	B45	0.80	0.055	24°	0.04
17	B30	0.20	0.070	18°	0.08
18	B30	0.60	0.070	18°	0.16
19	B30	0.60	0.070	18°	0.08
20	B15	0.80	0.085	24°	0.12
21	B15	0.80	0.085	12°	0.04
22	B45	0.80	0.055	12°	0.12
23	B45	0.40	0.055	12°	0.04
24	B30	0.60	0.070	18°	0.08
25	B30	0.60	0.100	18°	0.08
26	B30	0.60	0.070	18°	0.08
27	B30	0.60	0.070	30°	0.08
28	B30	1.00	0.070	18°	0.08
29	B15	0.40	0.085	12°	0.04
30	B30	0.60	0.070	6°	0.08
31	B15	0.80	0.055	24°	0.04
32	B15	0.80	0.055	24°	0.12
33	B45	0.80	0.085	24°	0.12
34	B15	0.40	0.055	12°	0.12
35	B0	0.60	0.070	18°	0.08
36	B15	0.40	0.085	12°	0.12
37	B15	0.40	0.055	24°	0.12
38	B15	0.80	0.055	12°	0.04
39	B30	0.60	0.040	18°	0.08
40	B15	0.40	0.085	24°	0.04
41	B30	0.60	0.070	18°	0.08
42	B45	0.80	0.055	12°	0.04
43	B30	0.60	0.070	18°	0.08
44	B15	0.80	0.085	12°	0.12
45	B45	0.80	0.085	24°	0.04
46	B30	0.60	0.070	18°	0.08
47	B60	0.60	0.070	18°	0.08
48	B15	0.40	0.055	24°	0.04
49	B15	0.80	0.085	24°	0.04
50	B30	0.60	0.070	18°	0.00

Maximize: Torque (Nm), BP (Kw), BMEP (bar), BTE (%), Mechanical efficiency (%), Volumetric efficiency (%)
Minimize: SFC (kg/kWh), CO (%). HC (ppm), NOx (ppm)

Experiments with a water-cooled, CRDI-compressed, single-cylinder engine featuring a tunable CR are depicted in Fig. 3. This was accomplished by adjusting the type of fuel blend, FIP, fuel IT, EL, and EGR rate according to a previously developed design matrix [1] while at the same time keeping the engine speed at 1500 rpm and the CR at 18. Table 2 details the instruments present in the experimental setup for gauging the air/fuel ratio, combustion pressure, crank angle, and applied load. These discovered signals are then sent to the computer via an interface using a high-speed data collection mechanism [3]. In addition to two fuel tanks, the setup includes an air box, manometer, fuel measuring unit, transmitters, piezo power supply, rotameter, calorimeters, and a process indicator, accompanied by a separate panel box. The components of the fuel injection system-such as fuel injectors, diesel injection unit, common rail equipped with a rail pressure gauge, pressure regulating valve, crank position sensor, wiring harness, and fuel pump-are controlled by

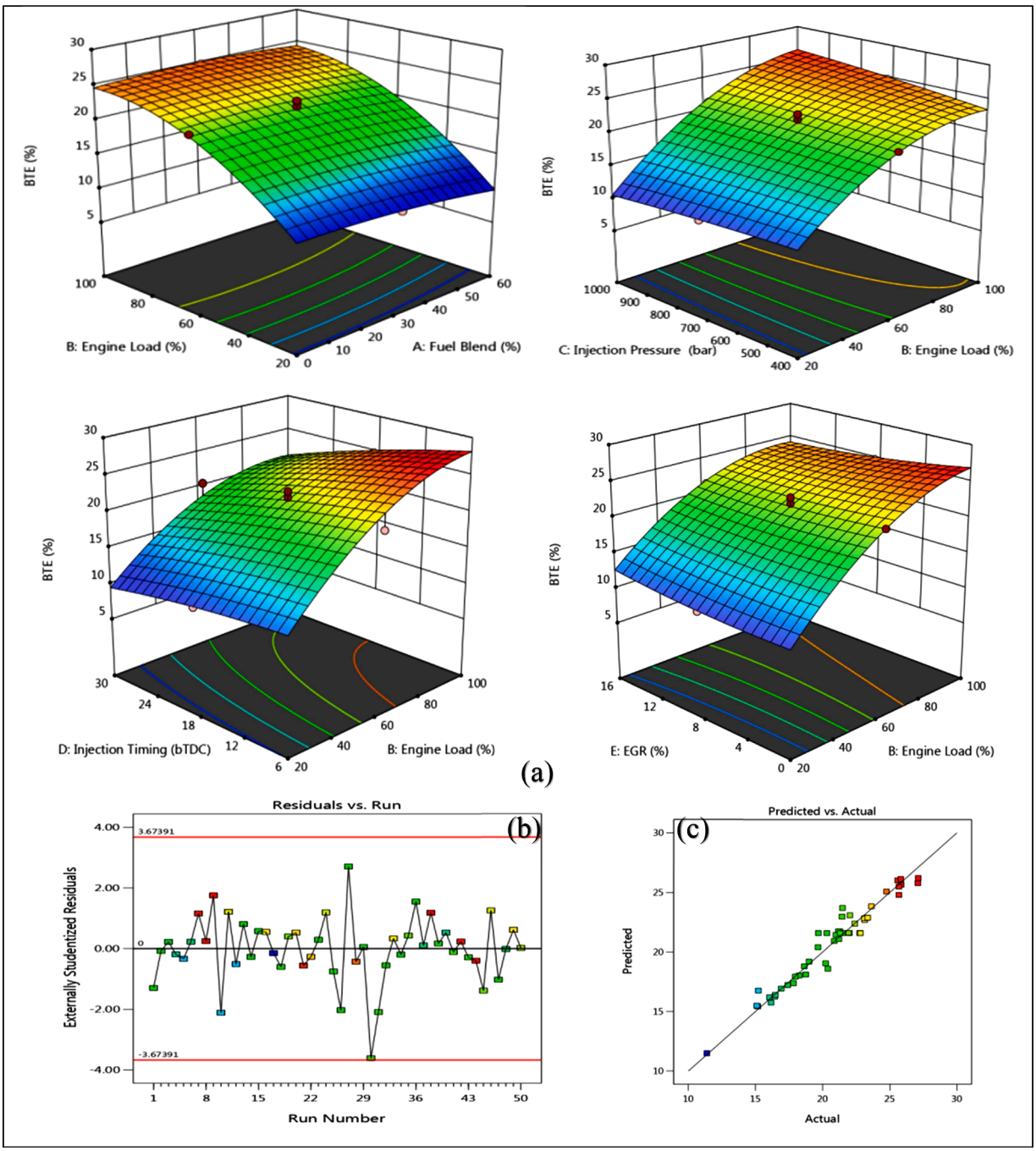

Fig. 4. **(a)** interactive effect of input parameters on BTE, (b) residuals vs run, (c) Predicted vs actual.

an open, customizable computer control unit. Apex Innovations improvements to engine software make it possible to track and record work progress, report data, and keep track of information about the various engine outputs. Exhaust emissions were analysed in a variety of situations, and pollutants were recorded using a gas analyzer. The experiment was conducted in an atmosphere, data collection commenced once the system had sufficiently stabilized, ensuring consistent and reliable measurements. An electronic control unit based on Nirai7r is responsible for monitoring and controlling everything other than the EL and EGR. The engine loads of 2.5 kg, 4.9 kg, 7.4 kg, 9.8 kg, and 12.3 kg were represented by applying loads of 20, 40, 60, 80, and 100%. By adjusting the control valve, we were able to implement water-cooled EGR. Eddy current dynamometer load is applied for varying EL 20 (2.5 kg) to 100% (12.3 kg). Strain gauge-type sensors are used, and the range of loads that can be applied is 0 to 50 kg. A piezo sensor with a low-noise cable is used to measure combustion pressure up to 35 MPa. Crank angle sensors are used for measuring the position of the crank with a resolution of 1 degree and a speed of 5500 RPM with a TDC pulse. The emission analysis instruments and their ranges are shown in Table 3. Based on the RSM design matrix, the experimental work is conducted by changing the input parameters of FB, EGR, FIP, EL, and FIT. Each combination of input parameter is adjusted in the CRDI engine based on Table 4a, and measurements are made after reaching steady state. Hence, using Sterculia Foetida biodiesel source, 50 combinations of experimentation were done and their result shown in Tables 19 and 20.

Table 5
ANOVA for BTE.

Source	SS	df	Mean Square	F-value	p-value	% Contribution
Model	568.1178	20	28.40589	25.58649	2.46E-13	Significant
Fuel Blend	3.64816	1	3.64816	3.286065	0.080235	0.608019
EL	461.6523	1	461.6523	415.8314	9.70E-19	76.90193
FIP	1.027203	1	1.027203	0.925248	0.344053	0.171578
FIT	64.94852	1	64.94852	58.50212	1.96E-08	10.81941
EGR	1.059503	1	1.059503	0.954343	0.336696	0.176575
AB	0.430128	1	0.430128	0.387436	0.538514	0.071646
AC	0.448878	1	0.448878	0.404325	0.529851	0.074778
AD	0.402753	1	0.402753	0.362778	0.551648	0.067099
AE	0.109278	1	0.109278	0.098432	0.755965	0.018207
BC	2.338203	1	2.338203	2.106127	0.157443	0.389799
BD	1.857628	1	1.857628	1.673251	0.206032	0.30984
BE	2.065528	1	2.065528	1.860516	0.183059	0.344822
CD	0.018528	1	0.018528	0.016689	0.898102	0.003082
CE	4.674153	1	4.674153	4.210224	0.049307	0.777931
DE	0.027028	1	0.027028	0.024345	0.87709	0.004498
A^2	0.676866	1	0.676866	0.609684	0.441234	0.112758
B^2	21.83614	1	21.83614	19.66881	0.000122	3.63812
C^2	0.067896	1	0.067896	0.061157	0.806419	0.011311
D^2	0.385881	1	0.385881	0.347581	0.560051	0.064283
E^2	0.443211	1	0.443211	0.399221	0.532442	0.073829
Residual	32.19554	29	1.110191			5.363895
Lack of Fit	22.40145	22	1.018248	0.727759	0.734982	3.731405
Pure Error	9.794088	7	1.399155			1.630824
Cor Total	600.3133	49				100

Table 6
analysis of variance for SFC.

Source	SS	df	Mean Square	F-value	p-value	% Contribution
Model	0.315855	20	0.015793	23.00358	1.00E-12	
A-Fuel Blend	0.004202	1	0.004202	6.121324	0.019451	1.250744
B-Engine Load	0.23716	1	0.23716	345.4451	1.19E-17	70.63728
C-Injection Pressure	0.00016	1	0.00016	0.233055	0.632892	0.059559
D-Injection Timing	0.02704	1	0.02704	39.38622	7.49E-07	8.0405
E-EGR	9.00E-05	1	9.00E-05	0.131093	0.719926	0.02978
Residual	0.01991	29	0.000687			5.926147
Lack of Fit	0.016922	22	0.000769	1.802267	0.216233	5.032758
Pure Error	0.002988	7	0.000427			0.893389
Cor Total	0.335765	49				100

4. Result and discussions of SF biodiesel fueled engine efficiency characteristics

Experimental work is done based on a design matrix of 50 input combinations made in design expert software, and the outcomes are plotted in the form of a 3-dimensional graph as shown below. The following graphs show the performance and emission characteristics of various blends of SF biodiesel under various operating conditions, such as varying engine load, fuel blend, FIP, fuel IT, and EGR. RSM graphs are plotted by varying any two of the input parameters, while keeping remaining three parameter at medium level for each output responses.

4.1. Interactive effect on BTE

Five input parameters were considered in the analysis, such as FB, EL, FIP, FIT, and EGR. The 3-dimensional surface graphs are plotted for any two parameters by keeping the remaining three influencing parameters as hold values at medium level as shown in Fig. 4. Engine load and FIT have more influence on BTE than the rest of the parameters considered. Generally, P-values less than 0.0500 are significant in ANOVA analysis. According to ANOVA data, engine load, injection timing, the interactive effect of injection timing, and EGR are more significant than the rest of the parameters. During the experimental investigations, reported values of BTE were 11.38% and 27.12% as minimum and maximum, respectively. When the engine operates under increasing load, it results in an enhancement of BTE. This is due to the fact that at high loads more heat is produced than at low loads, which in turn increases the BTE. This indicates that EL has a direct effect but other parameters such as FB, IP, IT, and EGR indirectly affect the BTE. No more significant variations were seen while varying the sterculia foetida biodiesel blends than diesel-fueled operations, but a slight decrease in BTE was reported at 60% of the fuel blend and 100% of EL operations due to the low energy of the biodiesel. Increasing FIP from 40 to 100 MPa resulted in an increase in BTE in more than half of load operations, but no considerable variations were seen below 50% of load operations. This is because a proper mix of air and fuel takes high IP and also produces high energy only at high loads. Injecting fuel nearer to TDC gives a higher BTE than injection too far away from TDC. Advancing IT from 6 to 30 degree before TDC results in a decrease in BTE. During the compression process, due to high pressure and temperature at injecting fuel near TDC leads to more complete combustion than earlier injection. The addition of EGR up to 16% from 0% results in an increase in BTE when operated at below 60% engine load but decreases beyond 60% to 100% of engine load operations. At low loads, the combustion process is inefficient compared to above half load, so the EGR stabilises or promotes the combustion process, but at high loads, already efficient combustion takes place, so adding EGR at high loads distracts from the efficient combustion process due to a lack of oxygen availability. This is because at high loads, more oxygen is required to meet energy requirements, which fails when introducing EGR in the combustion chamber. A second-order quadratic model has been developed to predict BTE by considering all parameters such as fuel blend, engine load, IP, IT,

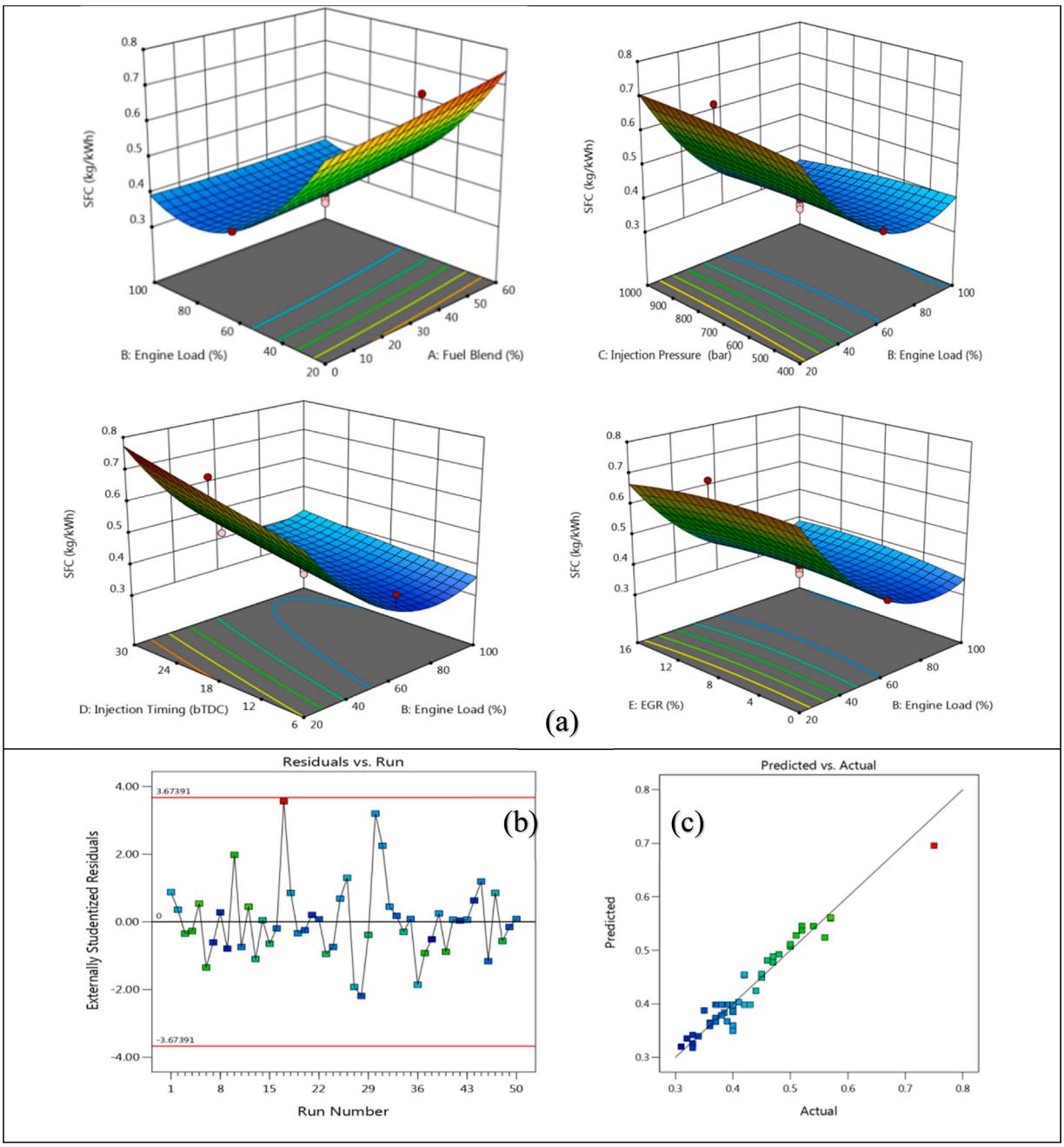

Fig. 5. (a) interactive effect of input parameters on SFC, (b) residuals vs run, (c) predicted vs actual.

and EGR. There was no huge difference between the predicted and actual values. Various influencing parameters are shown in the Table 5.

4.2. *Interactive effect on SFC*

Engine load increases resulted in a drastic decrease in SFC, but the trend started to increase above 80% of engine load, which is still lower

$$BTE = 11.9251 - 0.0560306xFB + 0.404561xEL - 0.00862806xFIP - 0.0285174xFIT - 0.362698xEGR + 0.000386458(FBxEL) + 5.26389e-05(FBxFIP) + 0.00124653(FBxFIT) - 0.000973958(FBxEGR) + 9.01042e-05(ELxFIP) - 0.00200781(ELxFIT) - 0.00317578(ELxEGR) + 2.67361e-05(FIPxFIT) + 0.000636979(FIPxEGR) - 0.00121094(FITxEGR) - 0.000646389xFB^2 - 0.00206516xEL^2 - 2.04722e-06xFIP^2 - 0.00305035xFIT^2 + 0.00735547xEGR^2$$

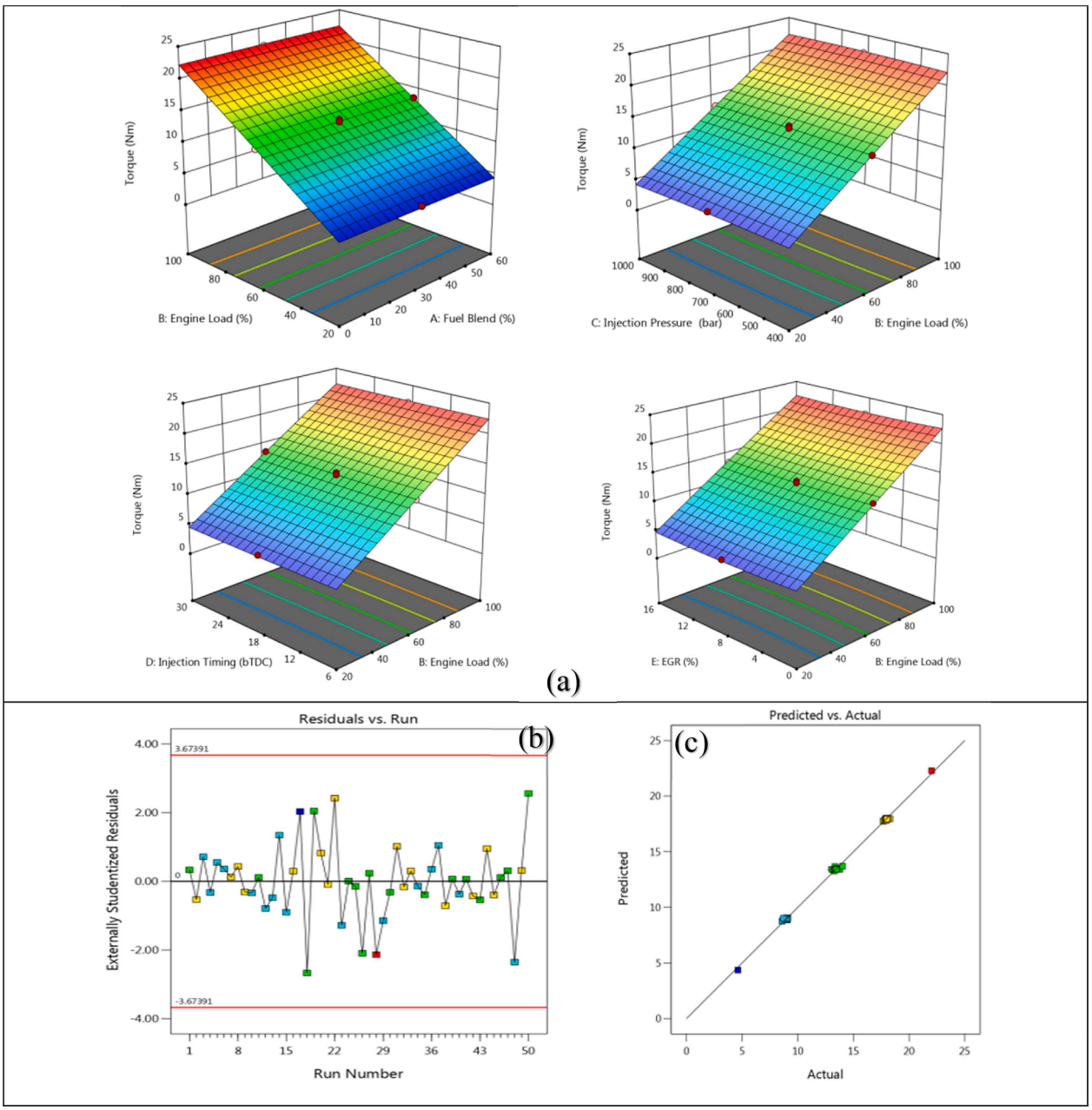

Fig. 6. (a) interactive effect of input parameters on Torque, (b) residuals vs run, (c) predicted vs actual.

than low-load operations. Addition of biodiesel with diesel in different proportions denoted as B0, B15, B30, B45, and B60. Compared to diesel fuel, the addition of biodiesel blends resulted in an increase in SFC at below half load operations, but beyond that load operation, there were no considerable changes seen between biodiesel and diesel fuel operations illustrated in Fig. 5. The lowest reported SFC during experimentation with 50 combinations of the proposed design matrix was 0.31 kg/kWh, and the highest SFC was 0.75 kg/kWh. The lowest fuel consumption was reported when engine settings were B15, 80% of EL, 55 MPa of IP, 12^{o} bTDC of injection, and 4% of EGR. The highest fuel consumption was reported at B30, 20% of engine load, 70 MPa of IP, 18 ^{o}bTDC of injection, and 8% of EGR. Increasing IP from 40 to 100 MPa resulted in a decrease in SFC at full load operations, but at low load operations, SFC started to increase slightly with the increase in IP. At low loads of operations, 40 MPa of FIP reported lower fuel consumption than 100 MPa of FIP. Generally, air availability at high loads is higher than at low loads in the combustion chamber; hence, insufficient air leads to incomplete combustion, which causes more SFC at low loads. The timing of fuel injection plays a vital role in SFC per unit of power output. Variations in IT from 6^{o}bTDC to 12^{o}bTDC, 18^{o}bTDC, 24^{o}bTDC to and 30 ^{o}bTDC result in an increase in SFC for all the considered loads of operations. Injecting fuel near the TDC gives better fuel consumption than the advanced IT of 30 ^{o}bTDC. During the compression process, the pressure and temperature of the air at the end of the compression process are higher than at the beginning of the compression process. Due to this, the fuel injected at high pressure in an atomized manner near the TDC leads to better mixing of fuel and air. This leads to a better combustion process with high BTE and low SFC. When the fuel is injected at the beginning of the compression stroke, partially fuels are combusted; hence, SFC increases with advanced injection. Addition of EGR at various proportions such as 0%, 4%, 8%, 12%, 16% and their results are shown as a surface graph. EGR addition above half load to full load results in an increase in SFC. But at low loads, the addition of EGR from 0 to 8% results in stagnant SFC, but beyond that, SFC starts to decrease

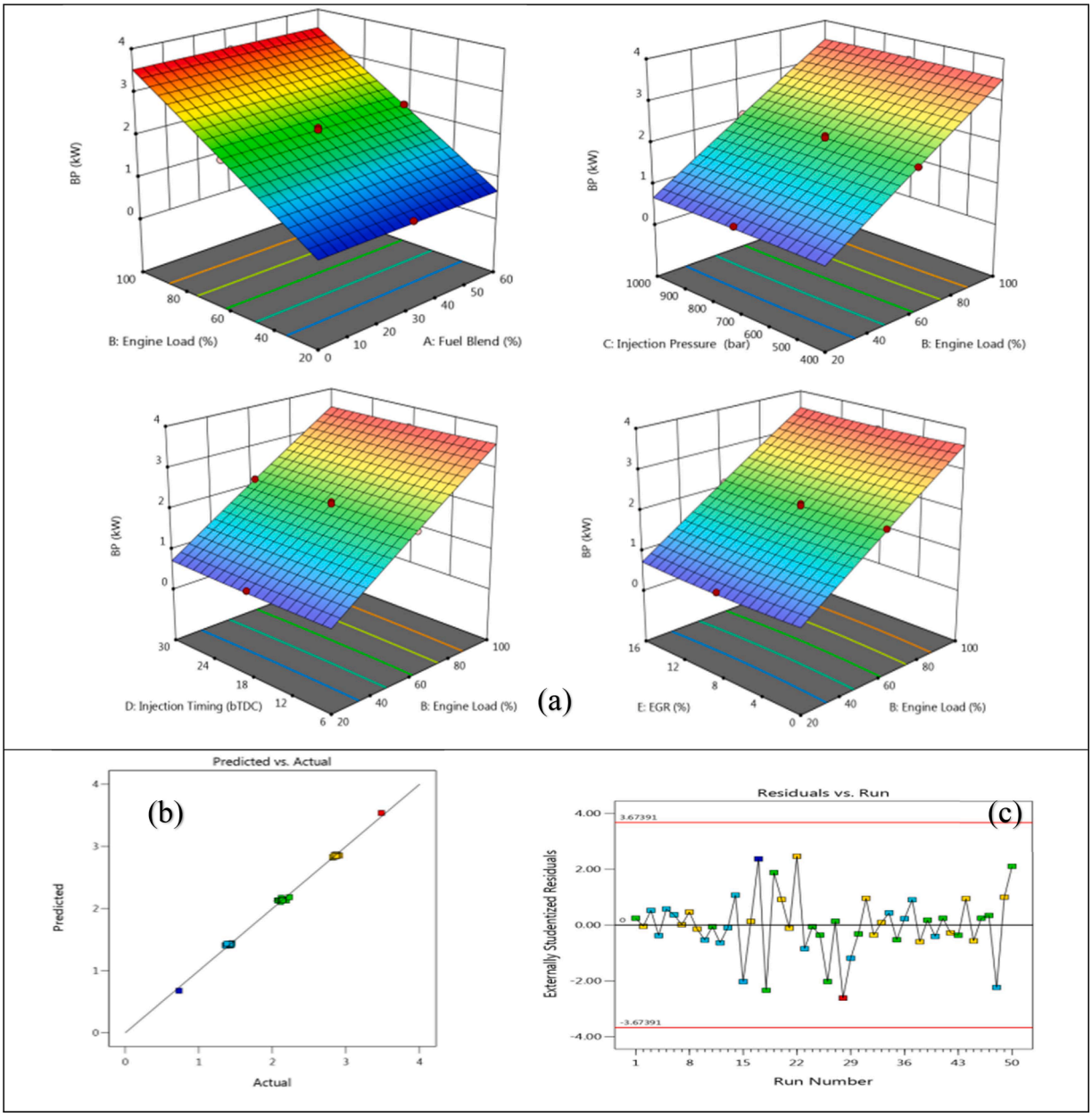

Fig. 7. (a) interactive effect of input parameters on BP, (b) predicted vs actual, (c) residuals vs actual.

due to the promotion of combustion. For predicting SFC, a model has been developed, and the predicted results are following the trends of actual values. Developed models are significant, and the lack of fit observed in the ANOVA was not significant is shown in Table 6. According to a p value less than 0.05 in the ANOVA table, the significant influencing parameters controlling SFC are identified as fuel blend, engine load, and FIT. The timing of fuel injection plays a vital role in SFC.

4.3. Interactive effect on torque

Torque, BP, and BMEP of a CRDI engine operated at a fixed speed of 1500 rpm are mainly dependent on or directly influenced by EL; notably, other input parameters considered have a very minimal effect on these output responses and indirectly affect the torque. The maximum ob-

$$SFC = 0.582164 + 0.00242778xFB - 0.0122937xEL + 0.000353889xFIP + 0.00646528xFIT + 0.009xEGR - 1.66667e-05(FBxEL) - 1.11111e-06(FBxFIP) - 1.38889e-05(FBxFIT) - 1.04167e-05(FBxEGR) - 1.875e-06(ELxFIP) - 4.6875e-05(ELxFIT) + 4.6875e-05(ELxEGR) - 6.94444e-07(FIPxFIT) - 1.25e-05(FIPxEGR) + 0.000104167(FITxEGR) + 6.11111e-06xFB^2 + 8.9375e-05xEL^2 - 7.77778e-08xFIP^2 + 2.08333e-05xFIT^2 - 0.000265625xEGR^2$$

tained values of torque, BP, and BMEP during the experimental run based on the design matrix are 22.02 Nm, 3.48 kW, and 4.18 bar. The lowest values obtained while conducting experimentation are 4.62 Nm, 0.73 kW, 0.88 bar of torque, BP, and BMEP. Second-order quadratic models have been generated with excellent levels of prediction accuracy. There is no considerable difference between predicted and actual values as shown in Figs. 6 to 8.

$$Torque = -0.647093 + 0.000494444xFB + 0.23843xEL + 0.00116278xFIP - 0.00469097xFIT - 0.0538542 xEGR + 3.125e-06(FBxEL) + 1.34722e-05(FBxFIP) - 0.000329861(FBxFIT) + 0.000130208(FBxEGR) -5.20833e-07(ELxFIP) - 0.000231771(ELxFIT) - 0.000363281(ELxEGR) + 2.95139e-05(FIPxFIT) +3.38542e-05(FIPxEGR) - 0.0011849(FITxEGR) - 5.63889e-05xFB^2 - 5.82812e-05xEL^2 - 1.64722e-06xFIP^2 + 0.000498264xFIT^2 + 0.00416797xEGR^2$$

$$BP = -0.126307 - 0.000658333xFB + 0.0393698xEL + 0.000191389xFIP - 0.000572917xFIT - 0.0134063xEGR + 3.125e-06(FBxEL) + 2.08333e-06(FBxFIP) - 3.125e-05(FBxFIT) + 5.20833e-06(FBxEGR) -7.29167e-07(ELxFIP) - 5.98958e-05(ELxFIT) - 3.51562e-05(ELxEGR) + 3.125e-06(FIPxFIT) +7.8125e-06(FIPxEGR) - 0.000117187(FITxEGR) - 5.27778e-06xFB^2 - 1.54687e-05xEL^2 - 2.19444e-07xFIP^2 + 0.000105903xFIT^2 + 0.000707031xEGR^2$$

$$BMEP = -0.0873569 - 0.000233333xFB + 0.0450823xEL + 0.000160556xFIP - 0.00110069xFIT - 0.0103958xEGR + 1.04167e-06(FBxEL) + 2.91667e-06(FBxFIP) - 7.29167e-05(FBxFIT) + 3.64583e-05 (FBxEGR) - 1.04167e-07(ELxFIP) - 3.90625e-05(ELxFIT) - 7.42188e-05(ELxEGR) + 5.90278e-06(FIPxFIT) +6.77083e-06(FIPxEGR) - 0.000221354(FITxEGR) - 9.16667e-06xFB^2 - 9.84375e-06xEL^2 - 2.86111e-07xFIP^2 + 9.89583e-05xFIT^2 + 0.000769531xEGR^2$$

$$Mech.Efficiency = 10.8839 - 0.279669xFB + 0.537674xEL + 0.0150236xFIP - 0.312365xFIT - 0.669219 xEGR + 0.00123646(FBxEL) - 5.68056e-05(FBxFIP) + 0.00205208(FBxFIT) + 0.00289063(FBxEGR) -0.000138646(ELxFIP) + 0.000888021(ELxFIT) + 0.00584766(ELxEGR) - 0.000146875(FIPxFIT) - 0.000257813(FIPxEGR) + 0.013138(FITxEGR) + 0.0021025xFB^2 - 0.00187203xEL^2 + 2.19444e-07x FIP^2 + 0.000831597xFIT^2 + 0.0103086xEGR^2$$

4.4. Interactive effect on BP

– Fig. 7

4.5. Interactive effect on BMEP

– Fig. 8

4.6. Interactive effect on Mechanical Efficiency

The mechanical efficiency depends on the lubrication effect of the fuel in the combustion chamber. Generally, fuels with low lubricating ability result in a decrease in mechanical efficiency; on the other hand, fuels with high lubrication result in a decrease in friction power. While using test fuels of diesel, SF biodiesel blended with diesel in various proportions, such as B15 (15% biodiesel+85% diesel), B30 (30% biodiesel+70% diesel), B45 (45% biodiesel+65% diesel), and B60 (60% biodiesel+40% diesel), has no significant changes in mechanical efficiency when considered throughout loads of operations at 1500 rpm in the CRDI engine. The maximum and minimum observed mechanical efficiency during the test were 13.84 bar and 40.58 bar, respectively. The boost pressure, such as 40 MPa to 100 MPa, has caused little variation in mechanical efficiency. An increase in pressure results in a slight increasing and decreasing trend in mechanical efficiency at low and high loads, respectively. At high loads, high FIP generates high temperatures by burning, which results in a decrease in efficiency. Variations of IT, such as 6 to 12, 18, 24, 30° bTDC at 1500 rpm in a common rail-type injection engine, affect the mechanical efficiency. The injection of fuel during the compression stroke at near TDC (6°bTDC) results in higher mechanical efficiency than early injection (30°bTDC). Advancing IT with high IP results in a bit of a decrease in mechanical efficiency for all loads of operations. Adding EGR (0%, 4%, 8%, 12%, and 16%) results in a slight decrease in mechanical efficiency at low loads and a slight

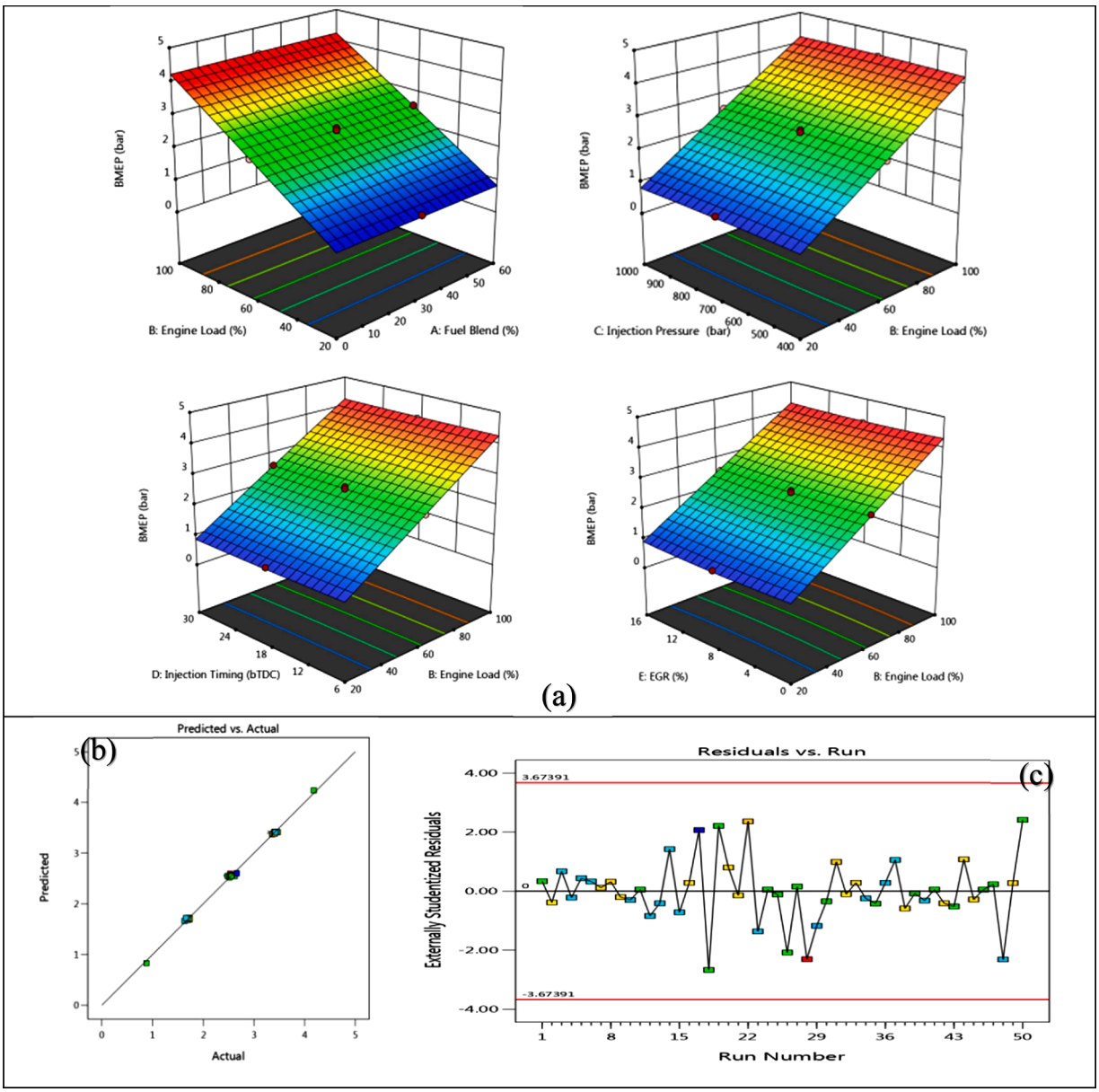

Fig. 8. (a) interactive effect of input parameters on BMEP, (b) Predicted vs actual, (c) residuals vs run.

increase in mechanical efficiency at high loads. At high loads, generally, the combustion temperature is high, which is reduced by the addition of EGR, resulting in improved mechanical efficiency. Based on ANOVA p value significance, the high to low order of influence on mechanical efficiency is EL, IT, and FB. Interactive effect of various factors on output responses are shown in Fig. 9.

4.7. Interactive effect on Volumetric Efficiency

The interactive effect of fuel blend and EGR and the interaction effect of FIT and EGR are higher than the rest of the interaction. According to ANOVA analysis, the significant factors affecting volumetric efficiency are engine load, fuel blend, injection timing, and EGR. Among these significant factors, the most influential parameters on vol. effi., are in the order EGR, IT, engine load, and fuel blend. An increase in engine load from minimum to maximum leads to a reduction in volumetric efficiency due to a lack of the required air-fuel proportions and time for mixing as shown in Fig. 10. An increase in fuel blends such as B15, B30, B45, and B60 leads to a reduction in volumetric efficiency, but up to 30% of fuel blends there is a slight increasing trend; beyond that, a decreasing trend is seen due to the low energy density and other properties of the prepared samples. During the operation, the maximum and minimum volumetric efficiency reported were 48.33% and 55.93%, respectively. The maximum efficiency was obtained when the engine settings were B30 as fuel, 60% load, 70 MPa IP, 18° bTDC, and 0% EGR addition. And the minimum volumetric efficiency was observed when the engine setting was B30, 60% of EL, 70 MPa of IP, 18°bTDC, and 16% of EGR. An increase in IP at high loads leads to an increase in volumetric efficiency due to better mixing of fuel-air, but at low loads poor combustion occurs, hence the increase in IP leading to a decrease in volumetric efficiency. Injection of fuel earlier in the compression stroke has a lower volumetric efficiency than injection of fuel nearer to TDC at the end of the compression stroke for all loads of engine operations because at near TDC of the compression process, the pressure and temperature of air are higher than at the start of the process. Based on the interactive effect of engine load and IT, at 30°bTDC and 100% EL, the volumetric efficiency is lowest, and at 6°bTDC and 20% EL, the volumetric efficiency is highest. For all loads of engine operations, adding EGR from

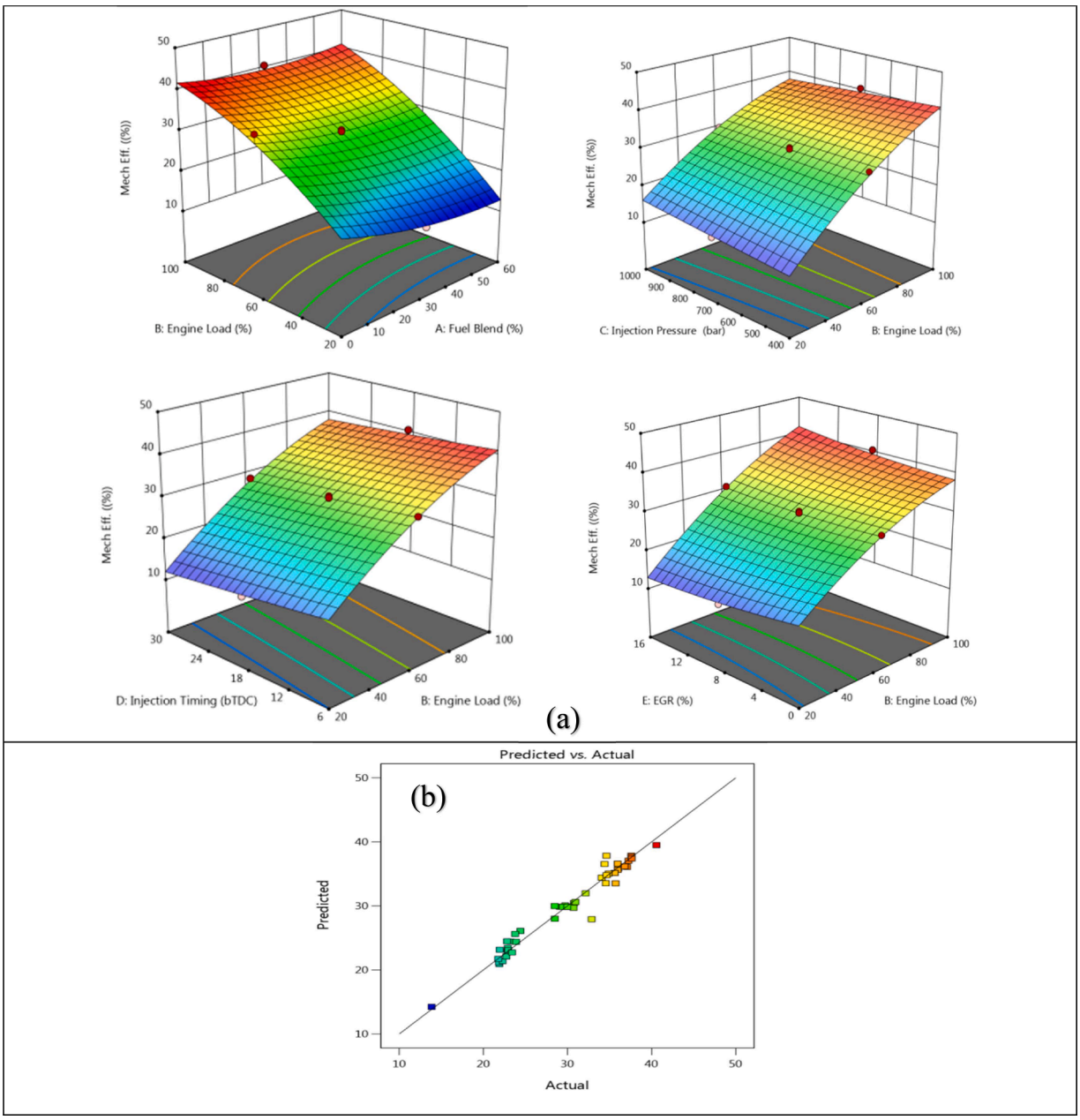

Fig. 9. (a) interactive effect of input parameters on mechanical efficiency, (b) predicted vs actual.

0 to 16% results in a drastic decrease in volumetric efficiency. Based on the interactive effect, 20% load and 0% EGR gave higher volumetric efficiency than 100% load and 16% EGR. Addition of EGR leads to poor air-fuel ratios because insufficient oxygen leads to incomplete burning of the supplied fuel, which decreases volumetric efficiency. Quadratic models were developed with reasonable prediction accuracy by considering all the input factors.

4.8. Combustion characteristics - cylinder pressure

In general, a pressure-crank angle diagram is one method for analysing the performance of a CRDI engine. The pressure inside the cylinder varies with crank angle. During the suction stroke, air is pulled into the cylinder, and the pressure is nearly flat for specific ranges of crank angle. The cylinder pressure rises quickly and creates a steep curve during the compression stroke. The injected fuel burns and produces high pressure and temperature throughout the combustion process.

$$VolumetricEfficiency = 61.6996 + 0.0372361xFB - 0.119786xEL + 0.0013425xFIP - 0.0772882xFIT - 0.645948x EGR - 8.22917e-05(FBxEL) - 1.65278e-05(FBxFIP) - 0.00155208(FBxFIT) + 0.00792187(FBxEGR) + 6.61458e-05(ELxFIP) +0.000736979(ELxFIT) + 0.00135547(ELxEGR) - 8.78472e-05(FIPxFIT) - 0.000369271(FIPxEGR) + 0.0112891(FITxEGR) -0.00125583xFB^2 + 0.000227969xEL^2 - 2.25e-07xFIP^2 - 0.00128646xFIT^2 - 0.00250391xEGR^2$$

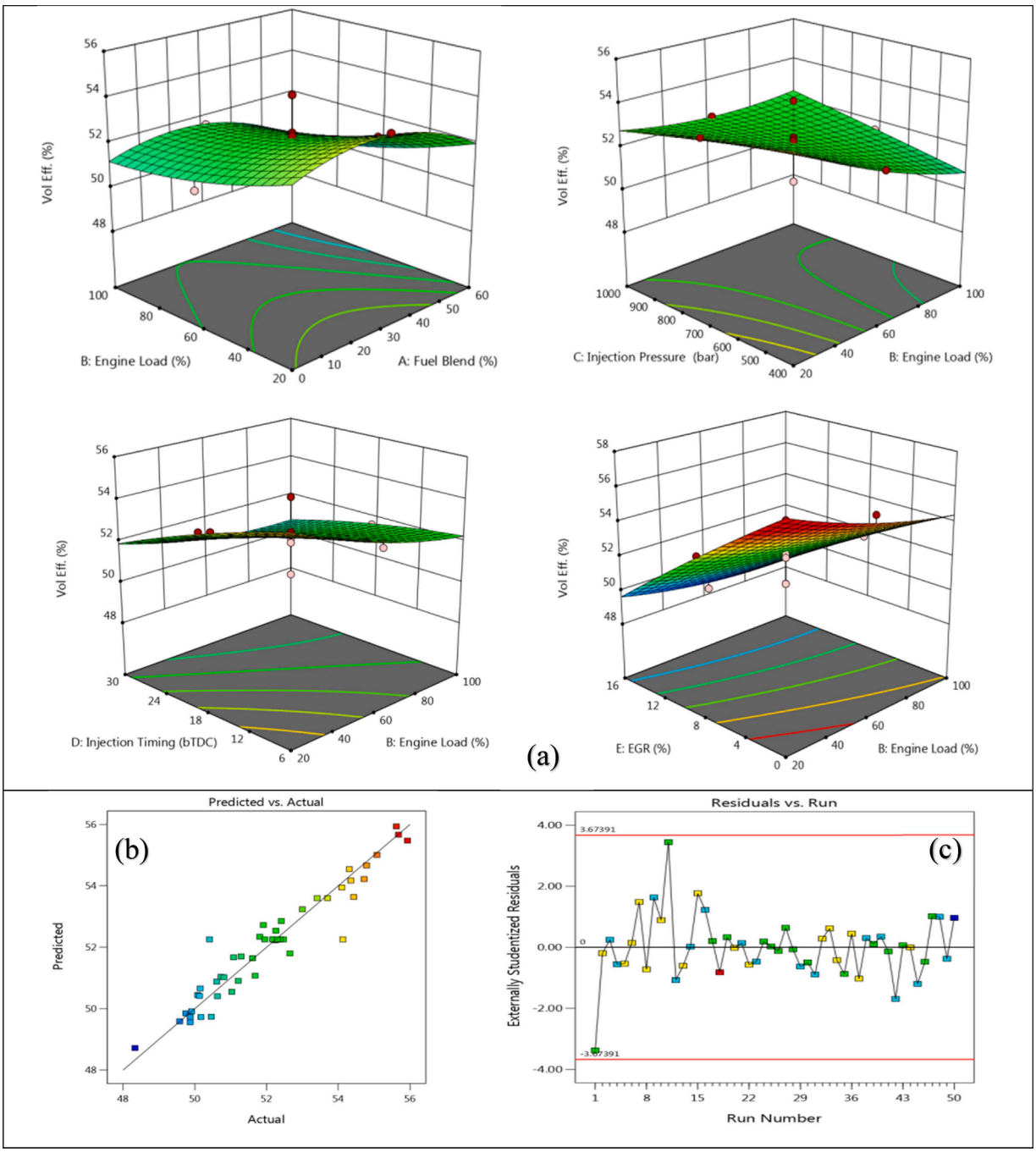

Fig. 10. (a) interactive effect of input parameters on vol. effi., (b) predicted vs actual, (c) residuals vs actual.

Because of the strong pressure force pushing the piston downward from TDC, pressure gradually falls due to the expansion process. During the exhaust stroke, the cylinder pressure approaches atmospheric pressure, so the pressure crank angle curve approaches flat once again.

When changing fuel blend B0, B30, B60 and keeping remaining parameters at mid-level and the corresponding responses on cylinder pressure is shown in Fig. 11. SFB (Sterculia foetida biodiesel) has the approximately nearer calorific value as diesel fuel. The addition of SFB to diesel enhances fuel quality by, for example, increasing the Cetane number, oxygen molecule content rises. A high Cetane number results in a shorter ID and faster combustion. As a result, at the end of the power stroke process, the peak cylinder pressure reported for B60 was higher than for B30 and diesel. The reported peak cylinder pressure for SFB B30 and B60 is higher than diesel.

4.9. Interactive effect on CO

As per ANOVA, the following parameters are significant on CO: engine load, IT, EGR, the interactive effect of EL and IT, and the interactive effect of FIT and EGR. Among these, the most influential factors on CO are IT, EL, and EGR. Increasing EL up to 60% results in a slight decrease to a stagnant effect on CO, but beyond 60% of load to full load, the CO emissions increase. At low load, addition of fuel blend results in decrease of CO than blended fuel supply at maximum load compare to diesel. This is because the required oxygen for burning is fulfilled by the blend itself at low loads. The maximum and minimum CO values observed during the experiment were 0.08% and 0.42% on a volume basis, respectively. An increase in FIP from 40 to 70 MPa results in a slight decrease in CO due to complete combustion caused by atomized droplets of fuel and air

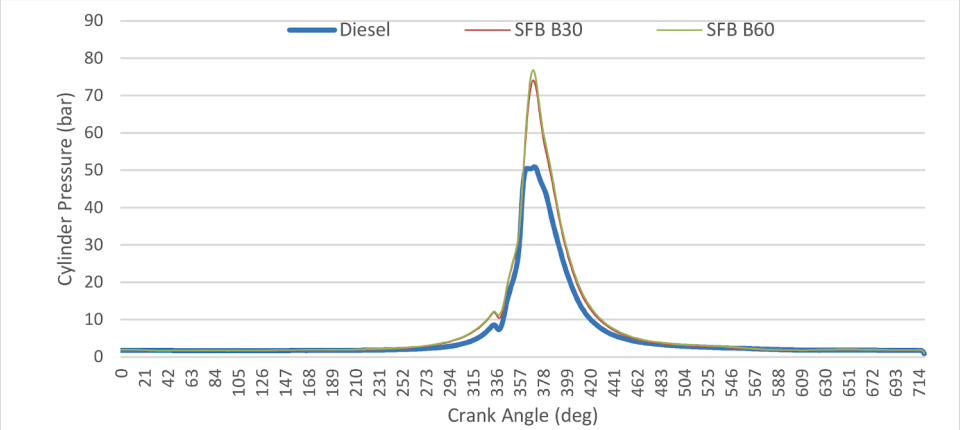

Fig. 11. crank angle versus cylinder pressure.

mixture, but beyond 70 MPa, up to 100 MPa of excessive pressure causes fuel droplets to become too small, which turns to incomplete combustion of injected fuel at considered size of engine, hence CO emission increases for all loads of operations. Very fine spray forms a gaseous state quickly and burns immediately without proper mixing with air, leading to incomplete combustion. Hence, optimum IP needs to be identified for reduced CO. Advancing IT from 6°bTDC to 12°bTDC, 18°bTDC, 24°bTDC and 30°bTDC results in enhancement of CO, specifically at low, 20% load, and the variations of IT effect is less than at maximum load of operations. CO is very high at high load and advancing IT to 30 degree. Near TDC injection during compression stroke results in better combustion due to better combustion efficiency leads to less waste of fuel hence CO emission decreases than at advanced injection of fuel during compression stroke due to incomplete combustion. Recirculating burned exhaust gases by 4%, 8%, 12%, and 16% into the combustion chamber leads to reduced oxygen presence, which causes incomplete combustion, and CO emissions are increasing. Up to 8% of EGR leads to a reduction of CO at low loads; beyond that, it starts to increase. In high loads, the addition of EGR from 0 to 16% results in an increase in CO due to a lack of oxygen as shown in Fig. 12. A model has been developed for forecasting CO by considering major influencing parameters.

$$CO = 0.746619 - 0.00648333xFB - 0.00953958xEL - 0.000460556xFIP - 0.0147431xFIT - 0.0283958xEGR + 3.33333^{-05}(FBxEL) + 2.5e-06(FBxFIP) + 2.77778^{-05}(FBxFIT) + 2.08333^{-05}(FBxEGR) - 4.16667^{05}(ELxFIP) + 0.000244792(ELxFIT) + 0.000132812(ELxEGR) + 1.38889e-06(FIPxFIT) + 2.08333e-06(FIPxEGR) + 0.000546875(FITxEGR) + 3.72222e-05xFB^2 + 4.28125e-05xEL^2 + 2.61111e-07xFIP^2 + 9.375e-05xFIT^2 + 0.000914062xEGR^2$$

4.10. Interactive effect on HC

Based on the ANOVA study, the most influential parameters on HC are fuel blend, engine load, and IT. The interactive effect of EL and IT is stronger on HC than the rest of the interactions is shown in Fig. 13. The highest and lowest HC emissions observed during experimentation were 64 ppm and 23.5 ppm on a volume basis, respectively. Engine load is one of the factors controlling the HC. It is found that up to 60% load, there is no significant effect on the HC, but beyond 60% load, the HC trend starts to increase due to improper air fuel composition. The addition of fuel blend up to 30% turns to a rise in HC due to insufficient oxygen for combustion, but beyond 30%, the HC emission starts to decrease for all loads of operations due to a sufficient amount of oxygen for the combustion process, which turns to complete combustion. Increasing IP from 40 to 100 MPa has no significant effect on HC, but at high loads, high IP leads to a slight decrease in HC due to the fine spray of injected fuel. But at low loads, increasing IP leads to a slight increase in HC due to inefficient combustion because of low air flow into the combustion zone. Early and later injections during the compression process are considered advanced TDC injection and near TDC injection. When IT goes earlier in the compression process, such as from 6 °bTDC to 12°bTDC, 18°bTDC, 24°bTDC, and 30°bTDC, it results in an increase in HC for all loads of operations. Because of insufficient oxygen, HC was higher with fuel injection advancement at high EL than at low EL. Based on the interactive effect of IT and EL, the maximum HC was seen at 100% EL and 30°bTDC of IT. The addition of EGR from 0 to 16% with an interval of 4% found that HC at high load was slightly decreasing trend due to efficient combustion than at low load. A quadratic model was developed for predicting the engine-out pollutant of HC with reasonable accuracy.

$$HC = 2.90028 + 0.455833xFB - 0.380625xEL + 0.0841944xFIP + 1.20486xFIT - 1.20312xEGR - 0.00270833(FBxEL) - 0.000333333(FBxFIP) + 0.0125(FBxFIT) + 0.025(FBxEGR) - 6.25e-05(ELxFIP) + 0.0161458(ELxFIT) - 0.00390625(ELxEGR) - 0.00194444(FIPxFIT) - 0.00125(FIPxEGR) + 0.0416667(FITxEGR) - 0.012xFB^2 + 0.00309375xEL^2 - 1.72222e-05xFIP^2 - 0.0107639xFIT^2 + 0.0539062xEGR^2$$

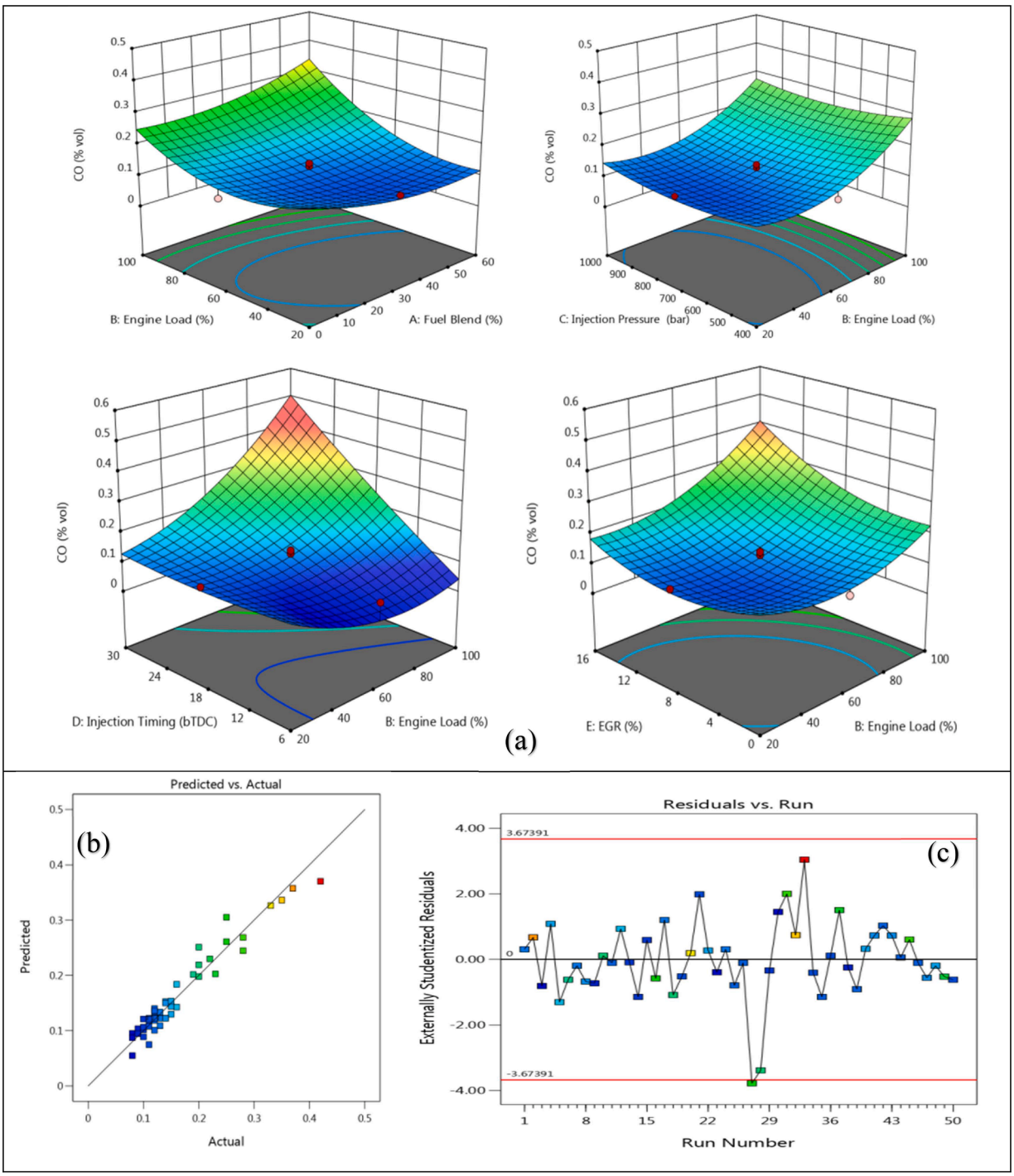

Fig. 12. (a) interactive effect of input parameters on CO, (b) predicted vs actual, (c) residuals vs run.

4.11. *Interactive effect on NOx*

Based on the ANOVA study of fuel blend, EL, IT, and EGR are significant terms, in the interactive effect of engine load and IT, and the interactive effect of EL and EGR, in the second order terms of fuel blend. Among these, the order of dominant influence on NOx was EGR, IT, EL, and fuel blends. Generally, the standard diesel engines are designed to perform better in a particular condition. The lowest reported NOx was 435 ppm at the setting of B30 fuel, 20% of EL, 70 MPa IP, 18 ^{o}bTDC of IT, and 8% of EGR, and the maximum NOx of 2063 was seen at B15 fuel, 80% of EL, 85 MPa IP, 24 ^{o}bTDC of IT, and 4% of EGR. Increases in engine load result in an increase in NOx up to 60% of load. From 60 to 80% of load operations, the resulted NOx was stagnant, but beyond 80% of load, the NOx reported had a decreasing trend. Coolant heat loss at high loads is higher than at low loads, which leads to low temperatures in the combustion zone and a decrease in NOx. Increasing the percentage of fuel blend results in a decrease in NOx, but up to 30% blend is approximately stagnant, and beyond 30% addition results in a decrease in NOx. Due to the low calorific value or energy density of blended fuel operations, NOx emissions were lower than in diesel-fueled operations. Increases in IP from 40 to 70 MPa result in a slight increase in NOx, but beyond 70 MPa of high IP operations, a slightly decreasing trend in NOx

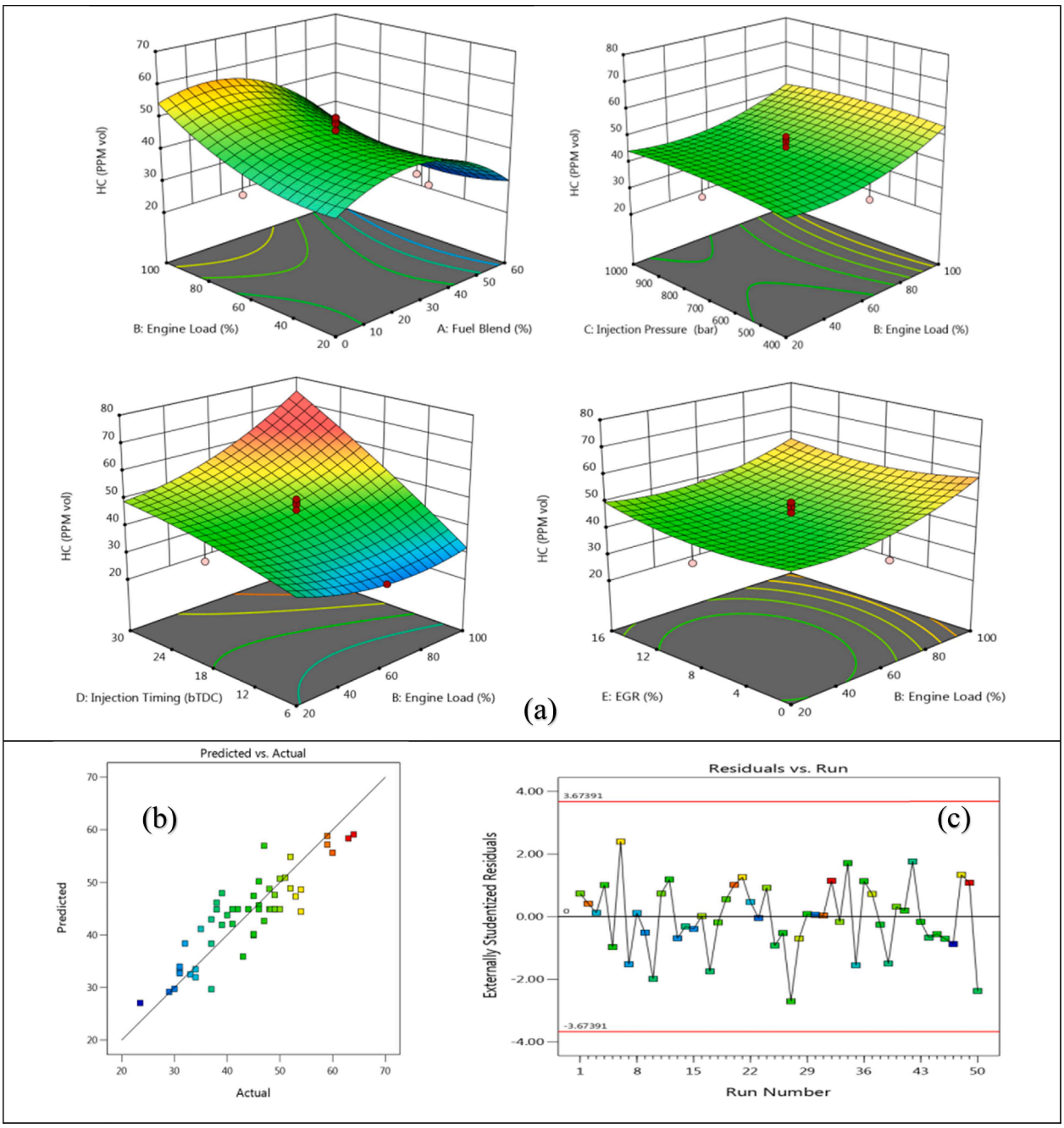

Fig. 13. (a) interactive effect of input parameters on HC, (b) predicted vs actual, (c) residuals vs run.

was seen due to more coolant heat loss and unfavorable conditions. At maximum load, the change in pressure from 40 to 100 MPa results in an increase in NOx due to better combustion caused by high IP. Varying the IT at different states during compression stroke causes variations in NOx. Compared to near TDC injection, the early injection of fuel during the compression stroke results in an increase in NOx due to less engine wall heat loss. Particularly at above 60% of load operations, the advanced IT causes a vigorous increase in NOx compared to below 50% load operations due to the high temperature is shown in Fig. 14. A model was developed for forecasting NOx output that was properly fitted with the actual data. Table 7–9 shows the ANOVA table for output responses. Table 12 shows percentage contribution of input factors on engine out responses.

$$NOx = -2024.18 + 7.45xFB + 41.3593xEL + 2.08939xFIP + 51.5462xFIT + 129.1xEGR + 0.00635417(FBxEL) - 0.00170833(FBxFIP) - 0.236458(FBxFIT) + 0.365104(FBxEGR) + 0.00313542(ELxFIP) + 0.669531(ELxFIT) - 0.998047(ELxEGR) + 0.00538194(FIPxFIT) - 0.0445313(FIPxEGR) - 0.428385(FITxEGR) - 0.162194xFB^2 - 0.323422xEL^2 - 0.00130528xFIP^2 - 1.40955xFIT^2 - 5.01523xEGR^2$$

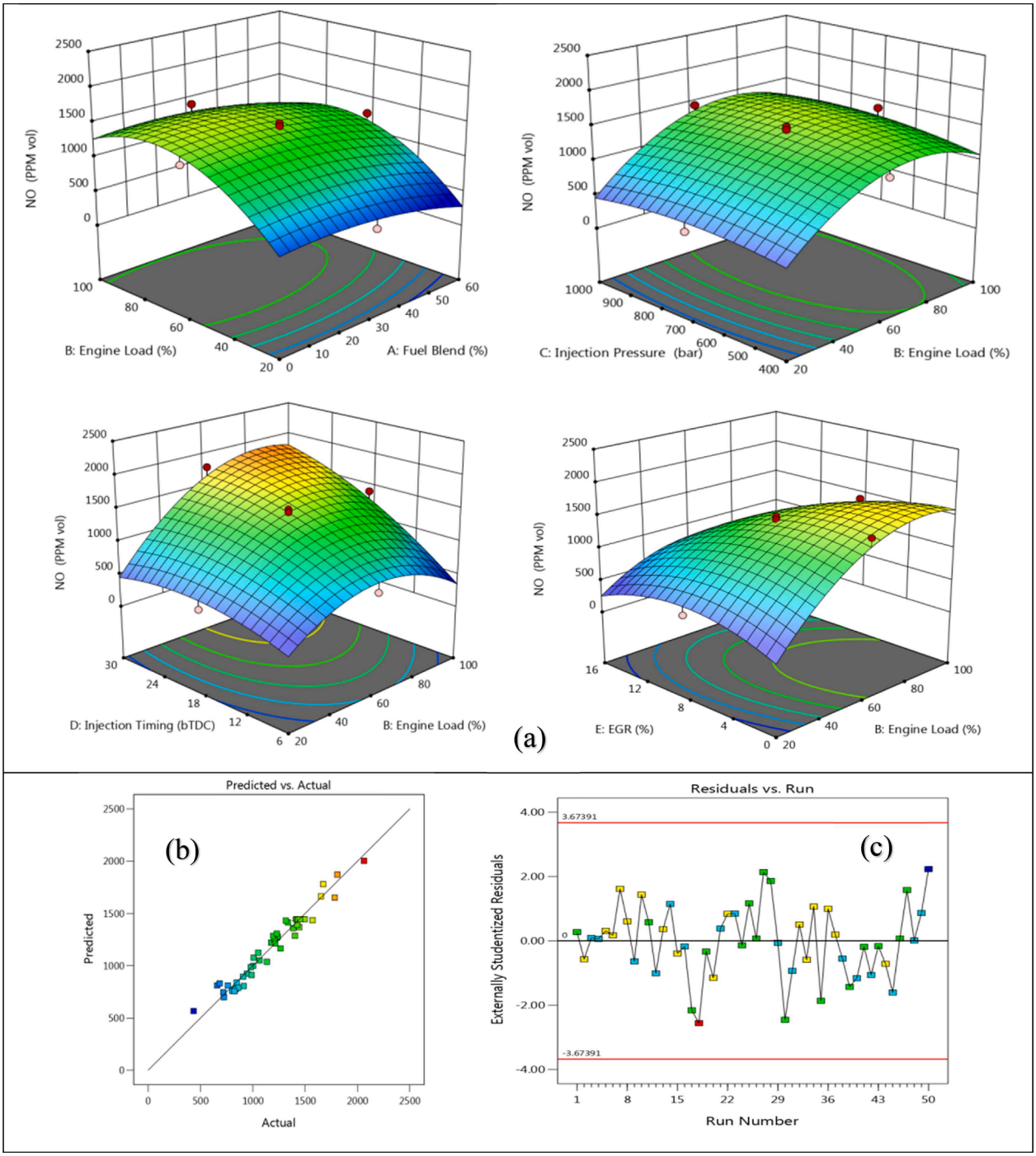

Fig. 14. (a) interactive effect of input parameters on NOx, (b) predicted vs actual, (c) residuals vs run.

Table 7
ANOVA for BTE, Mech. Effi., SFC.

Source	BTE		Mech. Effi.		SFC	
	F-value	p-value	F-value	p-value	F-value	p-value
Model	25.59	< 0.0001	35.72	< 0.0001	23	< 0.0001
FB	3.29	0.0802	13.05	0.0011	6.12	0.0195
EL	415.83	< 0.0001	663.91	< 0.0001	345.45	< 0.0001
IP	0.9252	0.3441	0.1355	0.7154	0.2331	0.6329
IT	58.5	< 0.0001	16.37	0.0004	39.39	< 0.0001
EGR	0.9543	0.3367	0.0304	0.8628	0.1311	0.7199
Lack of Fit	0.7278	0.735	19.11	0.0003	1.8	0.2162

5. RSM desirability approach for optimization

The composite desirability approach transforms individual responses into desirability function using Derringer-Suich methodology. RSM is a commonly used approach for designing the experimental design matrix of an IC engine to reduce the number of experiments and the time and resources required to find the optimum conclusions of a process [1]. The RSM statistical tool can handle multi-objective problems to give an efficient combination of input parameters for the process using the desirability approach [5,38]. Multiple output parameters are concurrently optimised using the desirability approach method. The basic

Table 8
ANOVA for torque, BP, BMEP.

Source	Torque		BP		BMEP	
	F-value	p-value	F-value	p-value	F-value	p-value
Model	1081.34	< 0.0001	868.95	< 0.0001	1067.62	< 0.0001
FB	0.8138	0.3744	0.1721	0.6813	0.5964	0.4462
EL	21615.32	< 0.0001	17369	< 0.0001	21340.89	< 0.0001
IP	0.0243	0.8773	0.3591	0.5537	0.0018	0.9661
IT	0.0151	0.9029	0.0021	0.9635	0.0902	0.7661
EGR	0.1244	0.7269	0.2571	0.6159	0.2227	0.6405
Lack of Fit	0.9683	0.563	1.12	0.4714	0.9	0.609

objective of the desirability technique is to identify the input parameter combinations that satisfy the requirements of each output response. By fitting a model of response surface to the data and calculating a score of overall desirability for each combination of input parameters, the combined RSM and desirability technique is used to optimise numerous output parameters [39–43]. The desirability approach transforms each response into a 0–1 scale. Generally, desirability 1 represents response desirability, less than 1 represents deviation from goal, and 0 represents undesirability of response. Based on the nature of the problem, generally the objective is to maximise, minimise, target, and keep within the range of responses. Based on the goal, weightage will optimise the result of a process from maximum to minimum. Generally, maximum desirability is considered a suitable, optimised result of a process. The objective of this work is to maximise the BP, torque, mech. effi., BMEP, vol. effi., and BTE and to minimise the SFC, CO, NOx, and HC.

The design matrix is prepared for experimental work based on identified influencing parameters with ranges such as FB (B0 to B60), EL (20 to 100%), FIP (40 to 100 MPa), FIT (6 to 30 degree bTDC), and EGR (0 to 16%). Generally, the central composite design (CCD)-based matrix gives more accurate results than box-behnken design; hence, the design matrix is prepared by following CCD. For a 5-parameter and 5-level CCD-based orthogonal design, 50 input combinations of 5 input parameters are given in the given ranges. 5 levels of input parameters used in the design matrix are shown in the Table 4. Randomised quadratic design matrix used for experimentation based on previous phase 1 work [1].

5.1. Optimisation analysis

A combined RSM and desirability approach is followed for optimisation of CRDI engine input parameter combinations to fulfil the goal of maximising output parameters of BTE, volumetric efficiency, mechanical efficiency, torque, BMEP, and BP and minimising SFC, CO, NO, and HC parameters. Parameter constraints and the weightage of individual parameters are shown in the Table 13. Individual desirability contributed by individual parameters to meet the optimisation goal is shown in the Table 13. Based on a maximum desirability of 0.973, optimised input combinations were obtained as B53 of Sterculia foetida biodiesel blends, 98% of EL, 100 MPa of FIP, FIT of 6^{o} bTDC, and 0% of EGR. At these optimised conditions, the actual observed output responses are shown in the Table 14. RSM fit statistics for various models are shown inTable 10 and 11.

5.2. ANN and RSM predictions

ANN is trained using the Levenberg backpropagation technique using experimental input and output data sets from an IC engine. With the help of a properly fitted regression model, 50 sets of input combinations and the matching output responses are each uniquely predicted. The Table 15, below displays the regression coefficients, hidden layer, and computation iterations for different output responses. ANN can evaluate hidden patterns in data more readily than RSM [4,40,44–46]. BTE, mechanical efficiency, SFC, volume efficiency, CO, HC, and NOx ANN prediction is better than RSM's projected goodness of fit by 1.35%, 1.79%, 4.36%, 2.39%, 7.30%, 17.18%, and 2.76%, respectively. This makes it obvious that ANN is a better option than RSM for predicting CRDI engine efficiency metrics. The illustration depicts the input, hidden layer, and output of an ANN shown in Fig. 15. Fig. 16 depicts an ANN regression model for CO, NOx, BTE, and SFC.

Table 11
RSM fit statistics of Mech. Effi., CO, HC, NOx.

	Mech. Effi.	CO	HC	NOx
R^2	0.961	0.8791	0.7699	0.956
Adjusted R^2	0.9341	0.7958	0.6113	0.9256
Predicted R^2	0.861	0.5233	0.1809	0.8265
Adeq Precision	25.1454	14.8887	8.4305	23.6829

Table 9
ANOVA for volumetric efficiency, CO, HC, NOx.

Source	Vol. effi.		CO		HC		NOx	
	F-value	p-value	F-value	p-value	F-value	p-value	F-value	p-value
Model	17.04	< 0.0001	10.55	< 0.0001	4.85	< 0.0001	31.47	< 0.0001
FB	7.17	0.0121	0.1983	0.6594	14.44	0.0007	20.18	0.0001
EL	20.76	< 0.0001	39.98	< 0.0001	7.27	0.0116	148	< 0.0001
IP	0.0024	0.9614	0.0079	0.9296	0.0465	0.8308	2	0.168
IT	29.4	< 0.0001	103.07	< 0.0001	53.75	< 0.0001	192.52	< 0.0001
EGR	247.03	< 0.0001	19.04	0.0001	0.0465	0.8308	110.89	< 0.0001
Lack of Fit	0.2832	0.9892	14.46	0.0007	3.51	0.0469	16.47	0.0004

Table 10
RSM fit statistics of BTE, SFC, BMEP, Vol. Effi., torque, BP.

	BTE	SFC	BMEP	Vol. Eff.	Torque	BP
R^2	0.9464	0.9407	0.9986	0.9216	0.9987	0.9983
Adjusted R^2	0.9094	0.8998	0.9977	0.8675	0.9977	0.9972
Predicted R^2	0.8357	0.7911	0.9957	0.8134	0.9957	0.9945
Adeq Precision	21.5615	22.2385	142.565	16.3855	143.478	128.615

Table 12
% Contribution of input factors on output parameters.

variable	BTE	Mech Effi.	SFC	Torque	BP	BMEP	Vol. effi.	CO	HC	NOx
FB	0.61	1.75	1.25	0.00	0.001	0.00	1.94	0.10	11.46	3.07
EL	76.90	89.3	70.64	99.81	99.76	99.83	5.61	16.66	5.76	22.47
IP	0.17	0.02	0.06	0.00	0.002	0.00	0.00	0.00	0.04	0.30
IT	10.82	2.20	8.04	0.00	1E-05	0.00	7.95	42.98	42.64	29.24
EGR	0.18	0.00	0.03	0.00	0.0015	0.00	66.79	7.93	0.04	16.84

Table 13
parameter constraints.

Variables	Objective	Threshold		Weightage		Priority	Desirability
		min	max	min	max		
BTE (%)	Maximize	11.38	27.12	1	1	3	1
Mech.Eff. (%)	Maximize	13.84	40.58	1	1	3	0.984
SFC (kg/kWh)	Maximize	0.31	0.75	1	1	3	0.951
Torque (Nm)	Maximize	4.62	22.02	1	1	3	1
BP (kW)	Maximize	0.73	3.48	1	1	3	1
BMEP (bar)	Maximize	0.88	4.18	1	1	3	1
Vol. eff. (%)	Maximize	48.33	55.93	1	1	3	1
CO (%)	Reduce	0.08	0.42	1	1	3	0.982
HC (ppm)	Reduce	23.5	64	1	1	3	0.867
Nox (ppm)	Reduce	435	2063	1	1	3	1
Combined desirability							0.973

Table 14
% difference between actual and RSM predicted optimum result.

Components	Predicted	Actual	% Error
Fuel Blend (%)	53.03	53.00	
Engine Load (%)	98.18	100.00	
Injection Pressure (MPa)	999.97	1000.00	
Injection Timing (^{o}bTDC)	6.00	6.00	
EGR (%)	0.00	0.00	
Torque (Nm)	22.19	22.00	0.86
BP (kW)	3.54	3.44	2.85
BMEP (bar)	4.22	4.09	3.09
BTE (%)	29.02	27.59	5.19
Mech. effi. (%)	40.22	41.70	3.56
SFC (kg/kWh)	0.33	0.31	5.82
Vol. Effi. (%)	55.79	53.70	3.89
CO (%)	0.13	0.13	3.41
HC (ppm)	23.50	24.00	2.08
NOx (ppm)	502.35	513.00	2.08

5.3. Meta-heuristic algorithm

The meta-heuristic implementation utilized real valued encoding with the following parameters shown in Table 16, 17.

The multi-dimensional performance analysis reveals close agreement among all optimization methods for primary objectives. RSM-CCD serves the reference standard, with meta-heuristic algorithms achieving comparable performance levels while maintain computational efficiency advantages. The comparative analysis demonstrates that all three meta-heuristic algorithms successfully replicated the RSM composite desirability optimization results with high fidelity shown in Table 18. PSO-DF achieved the highest similarity (97.9%) to RSM results, followed by DE-DF (95.3%) and GADF (88.9%).

All optimization methods converged toward similar operating conditions, validating the robustness of the optimization approach. The consistently high fuel blend ratios (52–53%), near maximum engine loads 97–98%), (0–0.5%) EGR and high IP (990–1000 bar) across all methods indicate these parameters are critical for achieving optimal multi objective performance

Uncertainty analysis

The experimental setup utilized the identical CRDI engine test rig as documented [37,47,48], ensuring consistent instrumentation and calibration standards. Instrumental uncertainties therefore remain unchanged, corresponding to ±0.5% (BTE), ±0.4% (BSFC). ±1% (EGR), ±0.2% (speed indication), ±0.3% (pressure sonsor), ±0.1% (dynamometer), ±0.3% (CO), ±0.6% (HC), AND ±0.8% (NOx). Total uncertainty comes below 2–5%

Conclusions

Empirical research is done in the water-cooled CRDI engine fueled with biodiesel blends derived from SF sources at a fixed compression ratio of 18 and speed of 1500 rpm by varying the main influencing parameters such as FIP, EGR, FIT and EL, the RSM desirability method used for optimization and the following conclusions are drawn:

- The Sterculia foetida seed oil extraction yield was calculated at 49–54%.
- The calculated biodiesel conversion yield was found to be 85% from Sterculia foetida seed oil by following the transesterification process.
- Biodiesel was produced following ASTM standards, and the analysis of the resulting fuel properties revealed that they conformed to the ASTM specification limits.
- The RSM experimental matrix, based on a central composite design comprising fifty input combinations, was developed using design expert software.
- RSM was applied both to predict and to develop second-order quadratic models for various engine output parameters investigated.
- Except EL, other parameters show comparatively minimal impact on these (Torque, BP, BMEP, Mech. Efficiency), at high IP operations

Table 15
comparisons of ANN and RSM prediction.

	BTE	Mech. Effi.	SFC	Torque	BP	BMEP	Vol. Effi.	CO	HC	NOx
Hidden Layer	4	3	5	4	2	2	15	5	13	12
Iterations	17	14	30	14	33	38	6	14	7	9
ANN R	0.9592	0.97	0.98	0.99	0.99	0.99	0.94	0.94	0.90	0.98
RSM R^2	0.9464	0.96	0.94	0.99	0.99	0.99	0.92	0.87	0.76	0.95
% Rise	1.35	1.79	4.36	0.06	0.08	0.06	2.39	7.30	17.18	2.76

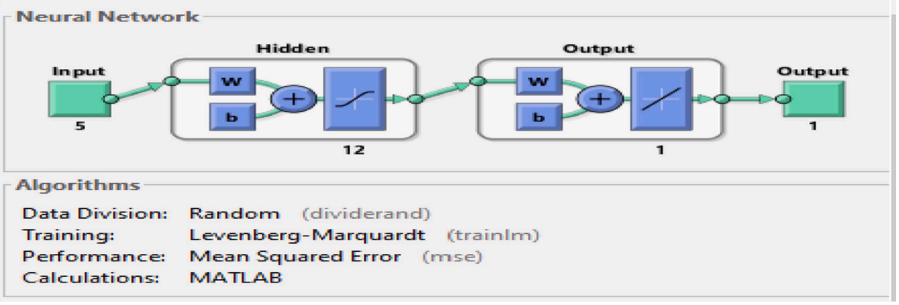

Fig. 15. ANN architecture.

these performance measures are predominantly influenced by EL when using any type of fuel.

- Based on high IP investigations, the EL and FIT play a more significant role in governing engine exhaust emissions and performance compared to the other parameters examined.
- Based on 40 to 100 MPa FIP operations, improved BTE is achieved due to fuel injection occurring near TDC at higher loads and during the early compression phase at lower loads.
- At low load conditions, the energy demand is sufficiently met using biodiesel blends alone under high FIP. However, beyond 55–60% operation, a slight reduction in BTE and an increase in SFC are observed, attributed to the lower energy density of biodiesel compared to conventional fuel.
- Overall, CRDI engine operations using sterculia foetida biodiesel blends as fuel showed that the best input combinations were B53 of sterculia foetida biodiesel blends, 98% of EL, 100 MPa of FIP, FIT of 6^{o} bTDC, and 0% of EGR, based on a maximum desirability of 0.973. ANN has the potential to predict engine output responses better than RSM.
- Sterculia foetida biodiesel blends fueled CRDI engine operations at high injection pressure, the EL has 77%, 89%, 70%, 99.9%, 5.61%, 16.66%, 5.76%, and 22.47% influence on BTE, mech. effi., SFC, torque, BP, BMEP, vol. effi., CO, HC, and NOx. IT has 11%, 8%, 8%, 43%, 42%, and 29% influence on BTE, SFC, Vol. eff., CO, HC, and NOx. EGR has 67%, 43%, 8%, and 17% influence on vol. effi., CO, and NOx. IP has 11.5% to 3% influence on HC and NOx.
- The prediction accuracy of ANN on CRDI engine output responses such as BTE, mechanical efficiency, SFC, volume efficiency, CO, HC, and NOx is 1.35%, 1.79%, 4.36%, 2.39%, 7.30%, 17.18%, and 2.76% higher than the response surface technique of prediction.
- All three meta-heuristic algorithms (GADF, DE-DF, PSO-DF) successfully replicated RSM composite desirability results with 88–98% similarity.
- Based on performance ranking, PSO-DF achieved highest similarity (97.9%), DE-DF provided fastest convergence, and GADF demonstrated good exploration capabilities.
- Optimal CRDI operation requires high blend ratios, near maximum loads, elevated injection pressures, and minimal EGR for maximum composite desirability.
- This study establishes meta-heuristic algorithm as viable alternatives for complex engineering optimization problems, offering enhanced flexibility while maintaining result accuracy comparable to established RSM methodologies.

Future research directions

- Investigate the synergistic effects of blending second-generation biofuels with third and fourth-generation biofuels, with emphasis on enhancing overall fuel quality, exploring oxygen enrichment strategies and evaluating the impact of advanced fuel additives on combustion, performance and emission characteristics at various operating speeds in diesel engines, with the objective of identifying optimum engine parameter settings.
- Deploying advanced optimization algorithm for predicting engine performance and determining optimal operational settings. Also, comparative analysis between conventional optimization methodologies to evaluate practical applicability in real time engine management systems.

Limitations of the study

The optimized engine parameter settings derived from this study are specifically valid for the experimental platform employed, namely CRDI engine operating at 1500 rpm with a CR of 18:1. The optimization outcomes and recommendations presented herein are constrained to the investigated ranges of input variables and their corresponding measured output responses.

The empirical equations developed through RSM exhibit reliable predictive accuracy only when the considered independent variables remain within experimental design space established in this investigation.

CRediT authorship contribution statement

Prakash Paramasivam: Writing – review & editing, Writing – original draft, Validation, Software, Resources, Methodology, Investigation, Formal analysis, Data curation, Conceptualization. **Dhanasekaran C:** Visualization, Supervision, Project administration, Funding acquisition.

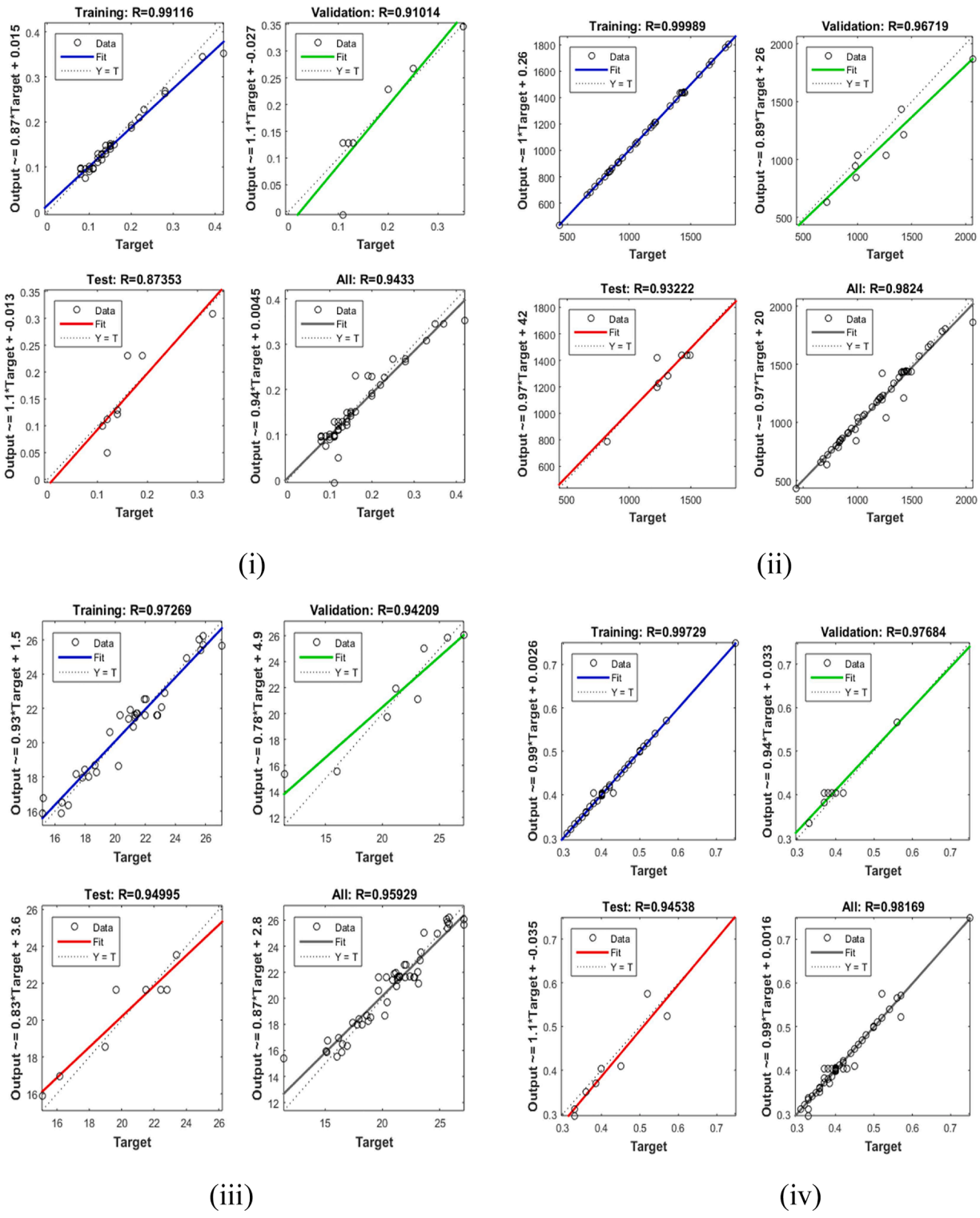

Fig. 16. ANN regression model of (i) CO, (ii) NOx, (iii) BTE, (iv) SFC.

Table 16
parameters of GADF and DE-DF.

Parameters	GADF	DE-DF
Population size	100 individuals	50
Generations	150	100
Crossover rate	0.8 (two point crossover)	0.8
Mutation rate	0.15 (Gausian)	0.7
Selection	Touranment selection (size 3)	Best/1/bin
Convergence	150 iterations	80 iterations

Table 17
parameters of PSO-DF.

Parameters	PSO-DF
Swarm size	40 particles
Iterations	150
Inertia Weight	0.9 towards 0.4 (linearly decresing)
Acceleration coefficients	$C_1 = c_2 = 2$
Convergence	120 iterations

Table 18
comparison of optimal input parameters from different optimization methods.

Methods	Fuel blend	Load	pressure	timing	EGR	Desirability score	Similarity to RSM
GADF	52.5 %	97.5 %	995 bar	6.2°	0.5%	0.8284	88.9
DE-DF	52.8%	98.0%	990 bar	6.1°	0.2%	0.8381	95.3%
PSO-DF	53.1%	97.8%	998 bar	6.0°	0.1%	0.8381	97.9%

Declaration of competing interest

The authors declare that they have no known competing financial interests or personal relationships that could have appeared to influence the work reported in this paper.

Acknowledgement

I thank my Guide and Vels University for support given to complete work in given timeframe.

Appendix

Table 19
Experimental results.

Exp. Run	Torque (Nm)	BP (kW)	BMEP (bar)	BTE (%)	SFC (kg/kWh)	Vol. effi (%)	CO (%)	HC (ppm)	Nox (ppm)
1	13.48	2.14	2.56	20.32	0.42	50.41	0.13	49	1469
2	17.67	2.82	3.36	20.87	0.41	49.75	0.37	59	1230
3	9.01	1.43	1.71	17.4	0.5	54.79	0.08	34	846
4	8.89	1.41	1.69	16.04	0.54	52.26	0.15	47	1003
5	8.97	1.42	1.7	15.17	0.57	50.61	0.16	46	945
6	9.11	1.45	1.73	16.44	0.52	49.87	0.19	54	907
7	17.91	2.85	3.4	25.68	0.33	50.46	0.13	32	914
8	18.08	2.88	3.43	25.85	0.33	50.08	0.14	33	803
9	17.94	2.86	3.41	27.09	0.32	54.43	0.09	31	1177
10	8.94	1.42	1.7	15.21	0.56	50.17	0.2	38	1135
11	13.44	2.13	2.55	22.78	0.38	54.13	0.12	49	1496
12	8.91	1.42	1.69	15.09	0.57	51.81	0.16	45	1008
13	8.99	1.43	1.71	18.74	0.46	50.73	0.1	31	724
14	9.08	1.44	1.73	18.99	0.45	55.68	0.1	37	989
15	8.87	1.36	1.69	17.83	0.48	52.65	0.1	31	719
16	17.95	2.85	3.41	23.13	0.37	51.68	0.25	51	1652
17	4.62	0.73	0.88	11.38	0.75	53.7	0.13	38	435
18	13.34	2.12	2.53	21.29	0.4	48.33	0.2	48	660
19	13.77	2.19	2.62	21.99	0.39	52.47	0.11	48	1415
20	17.95	2.86	3.41	23.28	0.36	49.58	0.33	60	1336
21	17.81	2.84	3.38	25.59	0.33	55.08	0.11	54	1386
22	18.28	2.91	3.47	23.63	0.36	50.13	0.15	34	829
23	8.75	1.39	1.66	18.25	0.47	54.31	0.08	29	839
24	13.42	2.13	2.55	22.76	0.38	52.38	0.13	50	1432
25	13.26	2.11	2.52	21.17	0.4	52.24	0.12	40	1444
26	13.06	2.07	2.48	19.68	0.43	52.18	0.12	42	1451
27	13.53	2.15	2.57	20.39	0.42	51.21	0.14	47	1783
28	22.02	3.48	4.18	24.76	0.35	51.61	0.2	52	1403
29	8.59	1.37	1.63	17.97	0.47	55.62	0.1	46	981
30	13.44	2.14	2.55	21.48	0.4	53	0.08	30	684
31	18.13	2.88	3.45	21.44	0.4	52.41	0.28	59	1808
32	17.77	2.82	3.38	21	0.4	49.87	0.35	64	1425
33	17.95	2.85	3.41	23.1	0.37	49.87	0.42	50	1238
34	8.91	1.42	1.69	18.64	0.45	50.81	0.11	43	862
35	13.26	2.11	2.52	21.93	0.385	51.29	0.12	35	1315.5
36	8.92	1.42	1.69	20.22	0.42	50.63	0.11	45	825
37	9.09	1.44	1.73	16.48	0.51	50.15	0.23	52	1065
38	17.87	2.85	3.4	27.12	0.31	54.1	0.09	41	1209
39	13.27	2.11	2.52	21.21	0.4	52.3	0.12	37	1194
40	8.93	1.42	1.7	16.16	0.52	54.35	0.15	49	1229
41	13.43	2.14	2.55	21.48	0.4	52.17	0.14	46	1428
42	17.95	2.86	3.41	25.68	0.34	51.91	0.12	37	1052
43	13.32	2.12	2.53	21.3	0.4	52.3	0.14	44	1430
44	17.96	2.87	3.41	25.82	0.33	49.91	0.12	39	762
45	17.93	2.84	3.41	22.03	0.39	51.08	0.28	45	1673
46	13.44	2.14	2.55	22.82	0.37	51.95	0.12	41	1451
47	13.465	2.14	2.555	19.655	0.44	51.03	0.14	23.5	1265.5
48	8.71	1.38	1.66	16.91	0.5	54.72	0.15	53	1215
49	17.99	2.87	3.42	23.36	0.36	53.41	0.22	63	2063
50	14.02	2.23	2.66	22.4	0.38	55.93	0.11	39	1571

Table 20
Experimental results of cylinder pressure at various crank angle for diesel, B30, B60 while constant parameters of EL (60%), FIP (70 MPa), FIT (18° bTDC), EGR (8%).

Crank Angle (degree)	Cylinder Pressure (bar)			Crank Angle (degree)	Cylinder Pressure (bar)		
	Diesel	B30	B60		Diesel	B30	B60
0	1.75	1.78625	1.93	360	46.44	48.4225	49.965
1	1.745	1.7875	1.93	361	48.955	53.05125	54.925
2	1.755	1.7925	1.935	362	50.12	57.375	59.555
3	1.76	1.795	1.94	363	50.465	61.34	63.815
4	1.765	1.80125	1.955	364	50.48	64.90875	67.665
5	1.765	1.8075	1.965	365	50.435	68.00375	70.985
6	1.765	1.8125	1.975	366	50.4	70.53375	73.625
7	1.765	1.815	1.975	367	50.395	72.41875	75.51
8	1.77	1.82	1.98	368	50.525	73.61	76.59
9	1.765	1.8225	1.985	369	50.765	74.06625	76.85
10	1.76	1.8225	1.98	370	50.955	73.775	76.28
11	1.76	1.8225	1.975	371	50.825	72.77875	74.985
12	1.76	1.8175	1.97	372	50.27	71.19375	73.14
13	1.76	1.8075	1.96	373	49.38	69.18625	70.94
14	1.765	1.8	1.94	374	48.37	66.91625	68.55
15	1.77	1.78875	1.925	375	47.45	64.54875	66.145
16	1.77	1.77625	1.905	376	46.69	62.24375	63.875
17	1.765	1.75875	1.895	377	46.045	60.13125	61.85
18	1.765	1.74	1.88	378	45.405	58.26	60.085
19	1.76	1.71625	1.87	379	44.695	56.60875	58.525
20	1.76	1.695	1.86	380	43.865	55.10875	57.09
21	1.76	1.6725	1.84	381	42.87	53.69875	55.71
22	1.76	1.64875	1.83	382	41.695	52.315	54.325
23	1.755	1.62875	1.81	383	40.38	50.92	52.9
24	1.755	1.61	1.795	384	39.005	49.48625	51.405
25	1.75	1.59	1.78	385	37.66	48.0125	49.855
26	1.75	1.57	1.765	386	36.38	46.49625	48.245
27	1.75	1.5525	1.75	387	35.185	44.94125	46.575
28	1.75	1.54	1.745	388	34.05	43.35875	44.88
29	1.75	1.5325	1.735	389	32.935	41.76	43.17
30	1.75	1.52875	1.73	390	31.82	40.16875	41.48
31	1.75	1.52125	1.72	391	30.705	38.6025	39.83
32	1.745	1.52	1.72	392	29.59	37.075	38.235
33	1.745	1.515	1.715	393	28.48	35.6025	36.72
34	1.735	1.51	1.71	394	27.39	34.19	35.285
35	1.73	1.50875	1.705	395	26.335	32.83625	33.94
36	1.725	1.50625	1.705	396	25.315	31.5475	32.66
37	1.725	1.5075	1.7	397	24.335	30.31	31.445
38	1.725	1.50375	1.69	398	23.39	29.12875	30.275
39	1.725	1.50625	1.69	399	22.485	27.99625	29.145
40	1.725	1.51	1.69	400	21.61	26.90375	28.055
41	1.725	1.51625	1.7	401	20.765	25.85	26.995
42	1.73	1.52125	1.705	402	19.945	24.83875	25.975
43	1.73	1.525	1.715	403	19.16	23.865	24.995
44	1.73	1.53125	1.72	404	18.395	22.9275	24.05
45	1.725	1.535	1.73	405	17.655	22.02625	23.14
46	1.725	1.53875	1.735	406	16.945	21.16125	22.255
47	1.72	1.54125	1.74	407	16.265	20.32875	21.41
48	1.715	1.54625	1.74	408	15.62	19.53625	20.595
49	1.715	1.55375	1.74	409	15	18.7775	19.82
50	1.715	1.55625	1.745	410	14.415	18.055	19.07
51	1.72	1.56125	1.75	411	13.86	17.37125	18.355
52	1.72	1.56625	1.745	412	13.34	16.72625	17.675
53	1.72	1.56875	1.745	413	12.845	16.1175	17.03
54	1.72	1.57125	1.75	414	12.375	15.545	16.42
55	1.72	1.575	1.75	415	11.93	15.00375	15.85
56	1.715	1.5775	1.745	416	11.52	14.48875	15.315
57	1.72	1.57875	1.745	417	11.13	14.005	14.805
58	1.71	1.57375	1.745	418	10.765	13.5425	14.33
59	1.71	1.5725	1.74	419	10.42	13.10125	13.88
60	1.71	1.56875	1.735	420	10.095	12.68375	13.44
61	1.71	1.56625	1.735	421	9.79	12.2825	13.02
62	1.715	1.56	1.735	422	9.5	11.89875	12.615
63	1.71	1.56125	1.73	423	9.22	11.53125	12.23
64	1.705	1.55875	1.73	424	8.955	11.17625	11.85
65	1.705	1.5575	1.735	425	8.7	10.84	11.495
66	1.705	1.5575	1.735	426	8.445	10.51875	11.15
67	1.705	1.555	1.735	427	8.21	10.20875	10.82
68	1.695	1.55	1.735	428	7.985	9.91125	10.5
69	1.695	1.5475	1.735	429	7.77	9.625	10.205
70	1.69	1.545	1.735	430	7.56	9.35125	9.92
71	1.69	1.5425	1.73	431	7.36	9.08625	9.645
72	1.695	1.54	1.73	432	7.17	8.835	9.385

(*continued on next page*)

Table 20 (*continued*)

Crank Angle (degree)	Cylinder Pressure (bar)			Crank Angle (degree)	Cylinder Pressure (bar)		
	Diesel	B30	B60		Diesel	B30	B60
73	1.695	1.5375	1.73	433	6.99	8.5925	9.13
74	1.7	1.5375	1.735	434	6.82	8.36375	8.89
75	1.705	1.53875	1.735	435	6.655	8.14875	8.665
76	1.705	1.54	1.735	436	6.5	7.94	8.445
77	1.715	1.545	1.74	437	6.35	7.74125	8.24
78	1.71	1.545	1.74	438	6.205	7.55125	8.05
79	1.705	1.54875	1.735	439	6.07	7.36625	7.86
80	1.705	1.54875	1.74	440	5.94	7.18625	7.675
81	1.705	1.5475	1.74	441	5.81	7.01375	7.505
82	1.705	1.545	1.74	442	5.69	6.85125	7.335
83	1.7	1.545	1.74	443	5.58	6.69125	7.175
84	1.7	1.54375	1.74	444	5.47	6.53625	7.015
85	1.7	1.54875	1.745	445	5.365	6.38875	6.855
86	1.695	1.55	1.745	446	5.27	6.2475	6.705
87	1.7	1.5475	1.755	447	5.175	6.11125	6.56
88	1.705	1.54625	1.755	448	5.08	5.97875	6.42
89	1.7	1.54375	1.755	449	4.99	5.85	6.285
90	1.7	1.54125	1.75	450	4.905	5.72625	6.16
91	1.705	1.54	1.745	451	4.82	5.60625	6.04
92	1.71	1.54125	1.74	452	4.74	5.49	5.925
93	1.71	1.54125	1.735	453	4.66	5.38125	5.815
94	1.71	1.54375	1.73	454	4.59	5.275	5.7
95	1.705	1.54625	1.72	455	4.52	5.17125	5.595
96	1.705	1.55	1.72	456	4.45	5.07375	5.5
97	1.7	1.55125	1.725	457	4.385	4.98125	5.395
98	1.7	1.55125	1.73	458	4.32	4.89125	5.3
99	1.695	1.55	1.73	459	4.26	4.80625	5.205
100	1.695	1.55	1.73	460	4.2	4.7225	5.11
101	1.69	1.54875	1.725	461	4.145	4.6425	5.03
102	1.695	1.55	1.73	462	4.095	4.56625	4.95
103	1.69	1.55125	1.735	463	4.045	4.49375	4.88
104	1.69	1.55	1.73	464	4	4.425	4.815
105	1.69	1.55	1.73	465	3.95	4.35625	4.745
106	1.685	1.5525	1.735	466	3.9	4.29	4.675
107	1.68	1.55125	1.74	467	3.85	4.22375	4.61
108	1.68	1.5525	1.74	468	3.805	4.16	4.55
109	1.68	1.5525	1.745	469	3.765	4.1025	4.49
110	1.69	1.55625	1.745	470	3.73	4.04625	4.43
111	1.69	1.55625	1.745	471	3.685	3.99375	4.375
112	1.69	1.5575	1.745	472	3.645	3.945	4.315
113	1.69	1.5625	1.745	473	3.605	3.89625	4.265
114	1.69	1.56125	1.75	474	3.57	3.85125	4.215
115	1.695	1.5625	1.755	475	3.54	3.80875	4.175
116	1.7	1.56375	1.755	476	3.51	3.7725	4.13
117	1.705	1.56625	1.755	477	3.48	3.73	4.09
118	1.705	1.56625	1.755	478	3.445	3.68875	4.05
119	1.705	1.5675	1.76	479	3.415	3.64625	4.015
120	1.71	1.5675	1.76	480	3.39	3.61	3.975
121	1.705	1.57	1.76	481	3.36	3.57125	3.94
122	1.71	1.57375	1.765	482	3.34	3.53625	3.9
123	1.705	1.57875	1.77	483	3.315	3.5	3.86
124	1.705	1.5825	1.77	484	3.29	3.47	3.825
125	1.71	1.585	1.775	485	3.26	3.435	3.79
126	1.71	1.5875	1.775	486	3.235	3.40625	3.76
127	1.71	1.59	1.775	487	3.205	3.37625	3.72
128	1.71	1.5925	1.78	488	3.18	3.3475	3.69
129	1.715	1.595	1.785	489	3.16	3.31875	3.66
130	1.715	1.59625	1.785	490	3.135	3.29125	3.635
131	1.71	1.6	1.79	491	3.11	3.265	3.605
132	1.71	1.60125	1.79	492	3.08	3.235	3.58
133	1.71	1.60875	1.795	493	3.065	3.2075	3.55
134	1.71	1.6125	1.8	494	3.045	3.18125	3.525
135	1.715	1.61375	1.805	495	3.025	3.15375	3.5
136	1.715	1.615	1.805	496	3.01	3.13125	3.47
137	1.71	1.615	1.81	497	2.99	3.10625	3.44
138	1.71	1.61625	1.815	498	2.97	3.0875	3.415
139	1.705	1.61625	1.815	499	2.955	3.06875	3.39
140	1.705	1.6175	1.815	500	2.94	3.05125	3.37
141	1.7	1.62125	1.815	501	2.92	3.03125	3.35
142	1.705	1.62375	1.815	502	2.905	3.01	3.33
143	1.705	1.62625	1.815	503	2.885	2.98875	3.32
144	1.705	1.6275	1.82	504	2.87	2.97	3.3
145	1.71	1.6325	1.82	505	2.85	2.95625	3.28
146	1.715	1.6375	1.825	506	2.84	2.93625	3.26

(*continued on next page*)

Table 20 (*continued*)

Crank Angle (degree)	Cylinder Pressure (bar)			Crank Angle (degree)	Cylinder Pressure (bar)		
	Diesel	B30	B60		Diesel	B30	B60
147	1.72	1.645	1.835	507	2.825	2.9225	3.245
148	1.715	1.65125	1.835	508	2.81	2.905	3.225
149	1.715	1.65375	1.845	509	2.8	2.89	3.21
150	1.715	1.6575	1.845	510	2.78	2.87625	3.195
151	1.72	1.65875	1.85	511	2.77	2.8625	3.185
152	1.73	1.66125	1.855	512	2.76	2.85	3.175
153	1.735	1.665	1.85	513	2.745	2.835	3.155
154	1.735	1.66875	1.855	514	2.73	2.82375	3.14
155	1.735	1.6725	1.855	515	2.715	2.80875	3.125
156	1.735	1.675	1.865	516	2.705	2.79625	3.11
157	1.73	1.67875	1.875	517	2.69	2.78125	3.09
158	1.73	1.68	1.885	518	2.675	2.7675	3.075
159	1.73	1.68	1.89	519	2.665	2.75375	3.06
160	1.73	1.685	1.895	520	2.655	2.74125	3.045
161	1.73	1.68625	1.905	521	2.645	2.73	3.03
162	1.735	1.69	1.905	522	2.635	2.72125	3.02
163	1.735	1.6925	1.9	523	2.625	2.71125	3.015
164	1.73	1.69375	1.9	524	2.615	2.705	3.005
165	1.725	1.6975	1.9	525	2.595	2.69625	2.995
166	1.72	1.6975	1.9	526	2.58	2.68875	2.985
167	1.725	1.70125	1.895	527	2.57	2.67875	2.975
168	1.725	1.70375	1.905	528	2.56	2.6675	2.965
169	1.725	1.70875	1.905	529	2.555	2.655	2.955
170	1.725	1.71625	1.915	530	2.545	2.6425	2.935
171	1.725	1.71875	1.92	531	2.535	2.6325	2.925
172	1.735	1.7225	1.92	532	2.525	2.62375	2.91
173	1.735	1.72375	1.92	533	2.515	2.61	2.89
174	1.735	1.725	1.93	534	2.505	2.59875	2.88
175	1.735	1.7275	1.93	535	2.5	2.58375	2.865
176	1.74	1.72875	1.935	536	2.485	2.56875	2.85
177	1.74	1.7325	1.935	537	2.47	2.5525	2.835
178	1.74	1.735	1.935	538	2.46	2.53625	2.815
179	1.745	1.73625	1.93	539	2.455	2.52	2.805
180	1.74	1.74	1.935	540	2.44	2.49875	2.785
181	1.745	1.74125	1.945	541	2.43	2.4825	2.77
182	1.745	1.745	1.95	542	2.42	2.465	2.745
183	1.74	1.7475	1.96	543	2.405	2.44625	2.72
184	1.735	1.75125	1.965	544	2.395	2.42625	2.695
185	1.735	1.75375	1.97	545	2.38	2.4025	2.68
186	1.735	1.7525	1.98	546	2.37	2.38	2.66
187	1.745	1.75625	1.975	547	2.365	2.36	2.64
188	1.75	1.75625	1.975	548	2.355	2.34	2.62
189	1.755	1.75625	1.97	549	2.35	2.32375	2.6
190	1.755	1.75875	1.97	550	2.335	2.3	2.585
191	1.755	1.7625	1.975	551	2.33	2.28125	2.56
192	1.76	1.7675	1.985	552	2.32	2.26	2.535
193	1.76	1.77125	1.985	553	2.31	2.24	2.505
194	1.755	1.775	1.995	554	2.3	2.21625	2.48
195	1.755	1.78125	2	555	2.29	2.195	2.45
196	1.75	1.7875	1.995	556	2.28	2.17125	2.425
197	1.75	1.79125	2	557	2.27	2.1525	2.405
198	1.76	1.7925	2.005	558	2.255	2.13375	2.375
199	1.76	1.795	2.01	559	2.25	2.11625	2.35
200	1.765	1.79625	2.015	560	2.24	2.1	2.33
201	1.76	1.795	2.01	561	2.225	2.08125	2.305
202	1.765	1.79625	2.01	562	2.215	2.06125	2.29
203	1.76	1.79875	2.005	563	2.2	2.03875	2.27
204	1.77	1.79875	2	564	2.185	2.02	2.255
205	1.775	1.805	2.005	565	2.17	1.99625	2.235
206	1.775	1.81	2.005	566	2.155	1.9775	2.21
207	1.775	1.815	2.01	567	2.145	1.96	2.19
208	1.78	1.81875	2.02	568	2.14	1.9425	2.165
209	1.785	1.82375	2.025	569	2.125	1.9275	2.14
210	1.785	1.8275	2.035	570	2.115	1.9125	2.12
211	1.785	1.82625	2.04	571	2.11	1.8975	2.1
212	1.785	1.82875	2.045	572	2.095	1.88125	2.085
213	1.785	1.8275	2.05	573	2.08	1.86625	2.075
214	1.79	1.83	2.05	574	2.075	1.84875	2.065
215	1.795	1.83375	2.06	575	2.06	1.83625	2.05
216	1.8	1.84125	2.06	576	2.055	1.82125	2.04
217	1.805	1.84875	2.065	577	2.05	1.81125	2.02
218	1.81	1.85625	2.075	578	2.04	1.80125	2.005
219	1.81	1.86375	2.09	579	2.035	1.79125	1.99
220	1.815	1.8725	2.1	580	2.025	1.78375	1.98

(*continued on next page*)

Table 20 (*continued*)

Crank Angle (degree)	Cylinder Pressure (bar)			Crank Angle (degree)	Cylinder Pressure (bar)		
	Diesel	B30	B60		Diesel	B30	B60
221	1.82	1.87875	2.11	581	2.015	1.7775	1.965
222	1.825	1.88375	2.12	582	2.005	1.76875	1.95
223	1.825	1.8925	2.125	583	1.995	1.75875	1.94
224	1.825	1.89875	2.135	584	1.995	1.75375	1.93
225	1.825	1.905	2.135	585	1.985	1.74375	1.925
226	1.83	1.91125	2.135	586	1.98	1.73375	1.91
227	1.825	1.92125	2.14	587	1.97	1.7275	1.9
228	1.825	1.92625	2.145	588	1.96	1.72	1.89
229	1.83	1.935	2.155	589	1.96	1.71125	1.88
230	1.835	1.94375	2.165	590	1.945	1.70375	1.875
231	1.84	1.95375	2.175	591	1.935	1.69625	1.86
232	1.845	1.965	2.185	592	1.93	1.69	1.845
233	1.855	1.97375	2.195	593	1.92	1.68125	1.84
234	1.865	1.98375	2.21	594	1.915	1.67125	1.83
235	1.87	1.995	2.22	595	1.91	1.6675	1.83
236	1.875	2.00375	2.225	596	1.905	1.66125	1.82
237	1.88	2.01375	2.235	597	1.9	1.655	1.815
238	1.885	2.025	2.25	598	1.895	1.65	1.81
239	1.895	2.0375	2.265	599	1.895	1.64375	1.805
240	1.895	2.05	2.275	600	1.885	1.64125	1.805
241	1.905	2.0625	2.29	601	1.88	1.63625	1.805
242	1.915	2.07625	2.305	602	1.87	1.62875	1.805
243	1.925	2.09	2.325	603	1.865	1.62375	1.8
244	1.93	2.10375	2.34	604	1.86	1.62125	1.8
245	1.94	2.11625	2.355	605	1.855	1.61875	1.8
246	1.94	2.13125	2.365	606	1.85	1.6175	1.8
247	1.95	2.145	2.375	607	1.85	1.6175	1.795
248	1.95	2.16125	2.385	608	1.845	1.6125	1.795
249	1.955	2.1825	2.4	609	1.845	1.61375	1.795
250	1.96	2.20375	2.415	610	1.845	1.61375	1.795
251	1.97	2.22375	2.435	611	1.84	1.61375	1.795
252	1.98	2.24375	2.455	612	1.84	1.61375	1.79
253	1.985	2.26375	2.475	613	1.84	1.6175	1.795
254	1.99	2.285	2.5	614	1.835	1.61875	1.795
255	2	2.30375	2.515	615	1.83	1.62625	1.8
256	2.01	2.3225	2.525	616	1.83	1.635	1.81
257	2.02	2.34375	2.55	617	1.825	1.6425	1.82
258	2.025	2.3625	2.575	618	1.815	1.65125	1.83
259	2.035	2.385	2.605	619	1.815	1.6625	1.84
260	2.05	2.41	2.63	620	1.815	1.675	1.85
261	2.06	2.43375	2.655	621	1.81	1.6875	1.86
262	2.07	2.45625	2.675	622	1.805	1.69875	1.87
263	2.08	2.4825	2.705	623	1.8	1.71	1.875
264	2.095	2.51	2.725	624	1.8	1.72125	1.88
265	2.11	2.53625	2.755	625	1.795	1.73125	1.885
266	2.125	2.5625	2.78	626	1.8	1.74375	1.89
267	2.135	2.5875	2.81	627	1.805	1.75625	1.905
268	2.155	2.615	2.84	628	1.805	1.76875	1.925
269	2.17	2.645	2.87	629	1.805	1.78125	1.94
270	2.185	2.6725	2.905	630	1.8	1.79125	1.96
271	2.2	2.70625	2.935	631	1.8	1.80125	1.97
272	2.225	2.73875	2.97	632	1.8	1.80875	1.98
273	2.24	2.77125	3	633	1.805	1.81625	1.985
274	2.255	2.80875	3.04	634	1.805	1.8225	1.995
275	2.275	2.845	3.08	635	1.815	1.8275	2
276	2.295	2.8825	3.125	636	1.82	1.83125	2.005
277	2.315	2.925	3.17	637	1.83	1.83625	2.01
278	2.325	2.96625	3.21	638	1.83	1.8375	2.015
279	2.35	3.0075	3.26	639	1.835	1.83875	2.02
280	2.375	3.05375	3.305	640	1.835	1.84375	2.025
281	2.405	3.09875	3.355	641	1.835	1.8475	2.03
282	2.425	3.14625	3.405	642	1.835	1.8525	2.04
283	2.455	3.19875	3.455	643	1.84	1.85375	2.035
284	2.48	3.25375	3.505	644	1.845	1.85375	2.035
285	2.505	3.31	3.565	645	1.845	1.855	2.04
286	2.53	3.37	3.63	646	1.85	1.855	2.04
287	2.56	3.43375	3.69	647	1.855	1.85375	2.035
288	2.6	3.495	3.76	648	1.85	1.8525	2.035
289	2.635	3.56	3.825	649	1.85	1.8525	2.03
290	2.67	3.6275	3.89	650	1.84	1.85125	2.03
291	2.71	3.69875	3.95	651	1.83	1.85125	2.03
292	2.75	3.77	4.015	652	1.835	1.855	2.035
293	2.795	3.84625	4.08	653	1.835	1.85375	2.035
294	2.835	3.92375	4.16	654	1.835	1.855	2.04

(*continued on next page*)

Table 20 (*continued*)

Crank Angle (degree)	Cylinder Pressure (bar)			Crank Angle (degree)	Cylinder Pressure (bar)		
	Diesel	B30	B60		Diesel	B30	B60
295	2.87	4.00375	4.245	655	1.83	1.8525	2.04
296	2.915	4.08875	4.33	656	1.83	1.85125	2.035
297	2.96	4.175	4.42	657	1.83	1.85	2.035
298	3.005	4.26375	4.51	658	1.835	1.85125	2.03
299	3.055	4.35375	4.61	659	1.835	1.85125	2.025
300	3.115	4.44875	4.71	660	1.83	1.85375	2.02
301	3.175	4.54875	4.81	661	1.83	1.85625	2.02
302	3.24	4.65	4.925	662	1.825	1.855	2.01
303	3.305	4.76	5.035	663	1.825	1.8575	2.01
304	3.375	4.8725	5.15	664	1.82	1.85875	2.005
305	3.45	4.9925	5.265	665	1.82	1.86	2.005
306	3.525	5.1175	5.39	666	1.82	1.86	2.005
307	3.605	5.25125	5.515	667	1.82	1.86	2.005
308	3.695	5.38875	5.65	668	1.825	1.8575	2.01
309	3.785	5.53375	5.79	669	1.825	1.855	2.01
310	3.875	5.68625	5.95	670	1.825	1.85	2
311	3.98	5.84625	6.115	671	1.83	1.84375	1.99
312	4.08	6.01	6.3	672	1.82	1.84	1.985
313	4.195	6.18125	6.475	673	1.81	1.835	1.98
314	4.315	6.36	6.665	674	1.81	1.8325	1.98
315	4.435	6.5475	6.855	675	1.805	1.825	1.98
316	4.57	6.7375	7.045	676	1.805	1.82	1.98
317	4.71	6.93125	7.245	677	1.795	1.81125	1.975
318	4.86	7.135	7.455	678	1.79	1.80375	1.97
319	5.01	7.35	7.67	679	1.79	1.795	1.965
320	5.175	7.575	7.905	680	1.785	1.78875	1.96
321	5.345	7.81375	8.145	681	1.79	1.77625	1.955
322	5.54	8.06625	8.405	682	1.785	1.7675	1.94
323	5.75	8.335	8.68	683	1.79	1.75625	1.925
324	5.975	8.615	8.97	684	1.79	1.745	1.905
325	6.205	8.91	9.265	685	1.79	1.73625	1.885
326	6.45	9.21	9.575	686	1.79	1.72625	1.87
327	6.705	9.52375	9.885	687	1.795	1.7175	1.86
328	6.98	9.8575	10.215	688	1.795	1.70875	1.855
329	7.28	10.2125	10.56	689	1.795	1.70375	1.855
330	7.6	10.585	10.92	690	1.785	1.69625	1.85
331	7.93	10.9725	11.3	691	1.78	1.69	1.845
332	8.26	11.355	11.685	692	1.78	1.6825	1.84
333	8.525	11.675	12.01	693	1.77	1.67125	1.83
334	8.61	11.80875	12.165	694	1.77	1.6625	1.825
335	8.415	11.63875	12.035	695	1.77	1.6575	1.815
336	7.985	11.1925	11.68	696	1.76	1.65	1.815
337	7.55	10.69	11.315	697	1.76	1.6425	1.805
338	7.325	10.38875	11.165	698	1.755	1.63875	1.805
339	7.435	10.445	11.35	699	1.755	1.63625	1.8
340	7.905	10.86125	11.845	700	1.755	1.63625	1.8
341	8.735	11.63375	12.61	701	1.755	1.6375	1.805
342	9.905	12.78125	13.675	702	1.75	1.64125	1.805
343	11.325	14.2675	15.035	703	1.75	1.6425	1.81
344	12.82	15.9625	16.605	704	1.745	1.6475	1.82
345	14.25	17.65625	18.2	705	1.745	1.64875	1.82
346	15.545	19.22625	19.715	706	1.745	1.6525	1.825
347	16.7	20.64625	21.11	707	1.745	1.65875	1.82
348	17.755	21.93875	22.4	708	1.745	1.6625	1.825
349	18.74	23.12875	23.6	709	1.74	1.67125	1.83
350	19.7	24.24875	24.745	710	1.74	1.68	1.835
351	20.665	25.3375	25.85	711	1.74	1.6875	1.85
352	21.68	26.43125	26.96	712	1.745	1.69875	1.865
353	22.79	27.57	28.11	713	1.75	1.70875	1.88
354	24.095	28.80125	29.36	714	1.75	1.72	1.895
355	25.835	30.26375	30.86	715	1.75	1.73	1.91
356	28.515	32.245	32.915	716	1.735	1.71625	1.89
357	32.445	35.1125	35.9	717	1.64	1.62875	1.79
358	37.42	39.0075	39.985	718	1.325	1.325	1.455
359	42.41	43.635	44.86	719	0.85	0.8525	0.935

Data availability

Data will be made available on request.

References

[1] P. Prakash, P.V. Elumalai, H. Chelladurai, G.R.N.R. Josephine, R. Velumayil, M. Asif, C.C. Kit, B. Venkatesan, S. Rajagopal, B. Sanjeevi, M.V. Reddy, P. S, Parameter fine tuning on CRDI engine operated with blends of grape biodiesel and

diesel, Case Stud. Therm. Eng. 60 (2024), https://doi.org/10.1016/j.csite.2024.104701.
[2] M. Gülüm, Prediction of exhaust gas temperature of a diesel engine running with diesel fuel-biodiesel-1-pentanol ternary blends, IOP Conf. Ser. Earth Environ. Sci. 1204 (2023) 012002, https://doi.org/10.1088/1755-1315/1204/1/012002.
[3] P. Prakash, C. Dhanasekaran, Influencing parameter optimisation of CRDI engine fuelled with lemongrass biodiesel blends, Int. J. Ambient Energy 44 (2023) 719–738, https://doi.org/10.1080/01430750.2022.2142286.
[4] P. Prakash, C. Dhanasekaran, Application of ANN, RSM on engine response prediction using lemongrass biomaterial blends, Mater. Today Proc. 69 (2022) 684–688, https://doi.org/10.1016/j.matpr.2022.07.116.
[5] J. Gamero-Salinas, J. López-Fidalgo, Response Surface Methodology using desirability functions for multiobjective optimization to minimize indoor overheating hours and maximize useful daylight illuminance, Sci. Rep. 15 (2025) 1–10, https://doi.org/10.1038/S41598-025-96376-X;SUBJMETA.
[6] D.K. Dond, R.R. Barshikar, H. Ghongade, A. Bhadre, S. Dond, Performance analysis of the CRDI diesel engine's performance and emission parameters blended with leftover cooking oil, additional nanoparticles, and hydrogen enrichment, Int. J. Appl. Mech. Eng. 30 (2025) 53–64, https://doi.org/10.59441/IJAME/195998.
[7] N. Indrareddy, K. Venkateswarlu, R. Konijeti, Experimental investigation of algae biofuel–diesel blends on performance of a CRDI diesel engine, Int. J. Ambient Energy (2020), https://doi.org/10.1080/01430750.2020.1725630.
[8] B. Balaji, V.B. A, Experimental investigation of a novel quaternary blend for CRDI engine: performance, emission, and combustion characteristics, Energy Sources A: Recovery Util. Environ. Eff. 44 (2022) 5729–5754, https://doi.org/10.1080/15567036.2022.2087803.
[9] D.K. Dond, N.P. Gulhane, Optimization of combustion parameters for CRDI small single cylinder diesel engine by using response surface method, J. Mech. Eng. Sci. 16 (2022) 8730–8742, https://doi.org/10.15282/jmes.16.1.2022.07.0690.
[10] D.K. Dond, N.P. Gulhane, Optimization of injection system parameter for CRDI small cylinder diesel engine by using response surface method, J. Inst. Eng. (India): C 102 (2021) 1007–1029, https://doi.org/10.1007/s40032-021-00688-6.
[11] B. Ashok, K. Nanthagopal, B. Saravanan, P. Somasundaram, C. Jegadheesan, B. Chaturvedi, S. Sharma, G. Patni, A novel study on the effect lemon peel oil as a fuel in CRDI engine at various injection strategies, Energy Convers. Manag. 172 (2018) 517–528, https://doi.org/10.1016/J.ENCONMAN.2018.07.037.
[12] M. Gülüm, A. Bilgin, A. ÇAKMAK, Production of the low viscosity waste cooking oil ethyl ester, Pamukkale Univ. J. Eng. Sci. 26 (2020) 674–682, https://doi.org/10.5505/PAJES.2019.48085.
[13] Optimization of transesterification of waste cooking oil with methanol by cubic spline interpolation on JSTOR, (n.d.). https://www.jstor.org/stable/27034654 (accessed January 10, 2026).
[14] P.K. Devan, N.V. Mahalakshmi, Performance, emission and combustion characteristics of poon oil and its diesel blends in a DI diesel engine, Fuel 88 (2009) 861–867, https://doi.org/10.1016/j.fuel.2008.11.005.
[15] P.K. Devan, N.V. Mahalakshmi, Study of the performance, emission and combustion characteristics of a diesel engine using poon oil-based fuels, Fuel Process. Technol. 90 (2009) 513–519, https://doi.org/10.1016/j.fuproc.2009.01.009.
[16] P.K. Devan, N.V. Mahalakshmi, Performance, emission and combustion characteristics of poon oil and its diesel blends in a DI diesel engine, Fuel 88 (2009) 861–867, https://doi.org/10.1016/J.FUEL.2008.11.005.
[17] F. Kusumo, T.M.I. Mahlia, A.H. Shamsuddin, A.R. Ahmad, A.S. Silitonga, S. Dharma, M. Mofijur, F. Ideris, H.C. Ong, R. Sebayang, J. Milano, M.H. Hassan, M. Varman, Optimisation of biodiesel production from mixed Sterculia foetida and rice bran oil, Int. J. Ambient Energy 43 (2022) 4380–4390, https://doi.org/10.1080/01430750.2021.1888802.
[18] M.B.P. Mangas, F.N. Rocha, P.A.Z. Suarez, S.M.P. Meneghetti, D.C. Barbosa, R. B. dos Santos, S.H.V. Carvalho, J.I. Soletti, Characterization of biodiesel and bio-oil from Sterculia striata (chicha) oil, Ind. Crops Prod. 36 (2012) 349–354, https://doi.org/10.1016/j.indcrop.2011.10.021.
[19] V.B. Marri, M.M. Kotha, A.P.R. Gaddale, Production process optimisation of Sterculia foetida methyl esters (biodiesel) using response surface methodology, Int. J. Ambient Energy 43 (2022) 1837–1846, https://doi.org/10.1080/01430750.2020.1723692.
[20] K. M. s, M. s, In situ acid catalysed transesterification of biodiesel production from Sterculia foetida oil and seed, 10.1080/15435075.2019.1671418 16 (2019) 1465–1474. 10.1080/15435075.2019.1671418.
[21] H.C. Ong, A.S. Silitonga, H.H. Masjuki, T.M.I. Mahlia, W.T. Chong, M.H. Boosroh, Production and comparative fuel properties of biodiesel from non-edible oils: Jatropha curcas, Sterculia foetida and Ceiba pentandra, Energy Convers. Manag. 73 (2013) 245–255, https://doi.org/10.1016/j.enconman.2013.04.011.
[22] M.S. Kavitha, S. Murugavelh, Optimization and transesterification of sterculia oil: Assessment of engine performance, emission and combustion analysis, J. Clean. Prod. 234 (2019) 1192–1209, https://doi.org/10.1016/J.JCLEPRO.2019.06.240.
[23] K.M. Sambasivam, S. Murugavelh, Optimisation, experimental validation and thermodynamic study of the sequential oil extraction and biodiesel production processes from seeds of Sterculia foetida, Environ. Sci. Pollut. Res. 26 (2019) 31301–31314, https://doi.org/10.1007/S11356-019-06214-7, 2019 26:30.
[24] D. Hari, T. Prasetiyo, N. Ilminnafik, A. Muhammad, The Effect of the transesterification process using KOH catalyst on the characteristics of biodiesel from Sterculia Foetida seeds as an alternative fuel, J. Keteknikan Pertan. 10 (2022) 253–267, https://doi.org/10.19028/JTEP.010.3.253-267.
[25] R. Bose, E. Bhattacharya, A. Pramanik, T.A. Hughes, S.M. Biswas, Potential oil resources from underutilized seeds of Sterculia foetida, L. - quality assessment and chemical profiling with other edible vegetable oils based on fatty acid composition, oxidative stability, antioxidant activity and cytotoxicity, Biocatal. Agric. Biotechnol. 33 (2021) 102002, https://doi.org/10.1016/J.BCAB.2021.102002.
[26] A.H. Sebayang, J. Milano, A.H. Shamsuddin, M. Alfansuri, A.S. Silitonga, F. Kusumo, R.A. Prahmana, H. Fayaz, M.F.M.A. Zamri, Modelling and prediction approach for engine performance and exhaust emission based on artificial intelligence of sterculia foetida biodiesel, Energy Rep. 8 (2022) 8333–8345, https://doi.org/10.1016/J.EGYR.2022.06.052.
[27] M. Vijay Kumar, M. Nandu, Evaluation of the performance and emission of diesel engine by using sterculia foetida biodiesel blend and DMC additive, Mater. Today Proc. 43 (2021) 191–195, https://doi.org/10.1016/J.MATPR.2020.11.620.
[28] M.T. Akhtar, M. Ahmad, A. Shaheen, M. Zafar, R. Ullah, M. Asma, S. Sultana, M. Munir, N. Rashid, K. Malik, M. Saeed, A. Waseem, Comparative study of liquid biodiesel from Sterculia foetida (bottle tree) using CuO-CeO2 and Fe2O3 nano catalysts, Front. Energy Res. 7 (2019) 433358, https://doi.org/10.3389/FENRG.2019.00004/BIBTEX.
[29] Y. Devarajan, D.B. Munuswamy, B.T. Nalla, G. Choubey, R. Mishra, S. Vellaiyan, Experimental analysis of Sterculia foetida biodiesel and butanol blends as a renewable and eco-friendly fuel, Ind. Crops Prod. 178 (2022) 114612, https://doi.org/10.1016/J.INDCROP.2022.114612.
[30] P.Karuppiah Subramanian, P. Muthiah, Development of functionalized heterogeneous catalyst from Ceiba pentandra stalk for biodiesel production using Sterculia foetida seed oil, Environ. Prog. Sustain. Energy 35 (2016) 308–314, https://doi.org/10.1002/EP.12203;SUBPAGE:STRING:ABSTRACT;REQUESTEDJOURNAL:JOURNAL:19447450;WEBSITE:WEBSITE:AICHE;JOURNAL:JOURNAL:15475921;WGROUP:STRING:PUBLICATION.
[31] Response surface methodology (RSM) in design of experiments - SixSigma.us, (n.d.). https://www.6sigma.us/six-sigma-in-focus/response-surface-methodology-rsm/(accessed January 11, 2026).
[32] Y. Raza, H. Raza, A. Ahmed, M.M. Quazi, M. Jamshaid, M.T. Anwar, M.N. Bashir, T. Younas, A.T. Jafry, M.E.M. Soudagar, Integration of response surface methodology (RSM), machine learning (ML), and artificial intelligence (AI) for enhancing properties of polymeric nanocomposites-A review, Polym. Compos. 46 (2025) 13591–13627, https://doi.org/10.1002/PC.30011;ISSUE:ISSUE:DOI.
[33] F.D.O. Riswanto, A. Rohman, S. Pramono, S. Martono, Application of response surface methodology as mathematical and statistical tools in natural product research, J. Appl. Pharm. Sci. 9 (2019) 125–133, https://doi.org/10.7324/JAPS.2019.91018.
[34] A. Reza, L. Chen, X. Mao, Response surface methodology for process optimization in livestock wastewater treatment: a review, Heliyon 10 (2024) e30326, https://doi.org/10.1016/J.HELIYON.2024.E30326.
[35] M. Kumar, R. Gautam, N.A. Ansari, Performance characteristics optimization of CRDI engine fuelled with a blend of sesame oil methyl ester and diesel fuel using response surface methodology approach, Front. Mech. Eng. 9 (2023) 1049571, https://doi.org/10.3389/FMECH.2023.1049571/BIBTEX.
[36] P. Kahhal, M. Ghasemi, M. Kashfi, H. Ghorbani-Menghari, J.H. Kim, A multi-objective optimization using response surface model coupled with particle swarm algorithm on FSW process parameters, Sci. Rep. 12 (2022) 2837, https://doi.org/10.1038/s41598-022-06652-3, 2022 12:1-.
[37] P. Prakash, P.V. Elumalai, H. Chelladurai, G.R.N.R. Josephine, R. Velumayil, M. Asif, C.C. Kit, B. Venkatesan, S. Rajagopal, B. Sanjeevi, M.V. Reddy, P. S, Parameter fine tuning on CRDI engine operated with blends of grape biodiesel and diesel, Case Stud. Therm. Eng. 60 (2024) 104701, https://doi.org/10.1016/J.CSITE.2024.104701.
[38] D.H. Lee, I.J. Jeong, K.J. Kim, A desirability function method for optimizing mean and variability of multiple responses using a posterior preference articulation approach, Qual. Reliab. Eng. Int. 34 (2018) 360–376, https://doi.org/10.1002/QRE.2258.
[39] P.R. Ganji, K.P. Chintala, V.R.K. Raju, S.R. Surapaneni, Parametric study and optimization using RSM of DI diesel engine for lower emissions, J. Braz. Soc. Mech. Sci. Eng. 39 (2017) 671–680, https://doi.org/10.1007/s40430-016-0600-0.
[40] V. Hariram, A. Bose, S. Seralathan, Dataset on optimized biodiesel production from seeds of Vitis vinifera using ANN, RSM and ANFIS, Data Brief 25 (2019) 104298, https://doi.org/10.1016/j.dib.2019.104298.
[41] A. Sharma, Y. Singh, A. Tyagi, N. Singh, Sustainability of the polanga biodiesel blends during the application to the diesel engine performance and emission parameters—Taguchi and RSM approach, J. Braz. Soc. Mech. Sci. Eng. 42 (2020), https://doi.org/10.1007/s40430-019-2102-3.
[42] P. Saiteja, B. Ashok, Study on interactive effects of CRDi engine operating parameters through RSM based multi-objective optimization technique for biofuel application, Energy 255 (2022) 124499, https://doi.org/10.1016/j.energy.2022.124499.
[43] M. Krishnamoorthi, R. Malayalamurthi, P.Mohamed Shameer, RSM based optimization of performance and emission characteristics of DI compression ignition engine fuelled with diesel/aegle marmelos oil/diethyl ether blends at varying compression ratio, injection pressure and injection timing, Fuel 221 (2018) 283–297, https://doi.org/10.1016/j.fuel.2018.02.070.
[44] S. Simsek, S. Uslu, H. Simsek, Proportional impact prediction model of animal waste fat-derived biodiesel by ANN and RSM technique for diesel engine, Energy 239 (2022) 122389, https://doi.org/10.1016/J.ENERGY.2021.122389.
[45] S. Simsek, S. Uslu, H. Simsek, Proportional impact prediction model of animal waste fat-derived biodiesel by ANN and RSM technique for diesel engine, Energy 239 (2022) 122389, https://doi.org/10.1016/j.energy.2021.122389.
[46] M. Aydın, S. Uslu, M. Bahattin Çelik, Performance and emission prediction of a compression ignition engine fueled with biodiesel-diesel blends: A combined

application of ANN and RSM based optimization, Fuel 269 (2020) 117472, https://doi.org/10.1016/j.fuel.2020.117472.

[47] M. Kumar, R. Gautam, N.A. Ansari, Performance characteristics optimization of CRDI engine fuelled with a blend of sesame oil methyl ester and diesel fuel using response surface methodology approach, Front. Mech. Eng. 9 (2023) 1049571, https://doi.org/10.3389/FMECH.2023.1049571/BIBTEX.

[48] P. Prakash, C. Dhanasekaran, Influencing parameter optimisation of CRDI engine fuelled with lemongrass biodiesel blends, Int. J. Ambient Energy 44 (2023) 719–738, https://doi.org/10.1080/01430750.2022.2142286;SUBPAGE:STRING:ACCESS.